A mechanism for telomere-specific telomere length regulation

Gabriela M. Teplitz [1*], Emeline Pasquier [1,2*], Erin Bonnell [1], Evelina De Laurentiis[1], Louise Bartle[1,3], Jean-François Lucier [4], Samantha Sholes [5,6,7], Carol W. Greider [5,8], Raymund J. Wellinger [1,$].

1: Department of Microbiology and Infectiology, Faculty of Medicine and Sciences, Université de Sherbrooke, Sherbrooke, Canada
2: Current Address: CNRS-UMR9019, Gustave Roussy Institute, Villejuif, France.
3: Current Address: School of Agriculture, Food and Wine, The University of Adelaide, Urrbrae, Australia
4: Department of Biology, Faculty of Sciences, Université de Sherbrooke, Sherbrooke Canada
5: Department of Molecular Biology and Genetics, Johns Hopkins University School of Medicine, Baltimore, USA.
6: Biochemistry, Cellular and Molecular Biology Graduate Program, Johns Hopkins University School of Medicine, Baltimore, USA
7: Current Address: Merck & Co., 770 Sumneytown Pike, West Point, USA
8: Department of Molecular Cell and Developmental Biology, University of California, Santa Cruz, USA

* The first two authors contributed equally to this work.

$ To whom correspondence should be addressed:
Email: Raymund.Wellinger@Usherbrooke.ca Tel: (819) 821 8000 ext 75214

Keywords: Telomere length maintenance, Telomeric chromatin, Telomerase recruitment, Ku-proteins, Telomerase RNA

Summary Paragraph:

Telomeric DNA, composed of short, direct repeats, is of crucial importance for chromosome stability. Due to intrinsic problems with replicating this DNA, the repeat tracts shorten at each cell division. Once repeat tracts become critically short, a telomeric stress signal induces cellular senescence and division arrest, which eventually may lead to devastating age-related degenerative diseases associated with dysfunctional telomers. Conversely, maintenance of telomere length by telomerase upregulation is a hallmark of cancer. Therefore, telomere length is a critical determinant of telomere function. How telomere length is established and molecular mechanisms for telomere-specific length regulation remained unknown. Here we show that subtelomeric chromatin is a determinant for how telomere equilibrium set-length is established in *cis*. The results demonstrate that telomerase recruitment mediated by the telomere-associated Sir4 protein is modulated on chromosome 3L in a telomere-specific way. Increased Sir4 abundance on subtelomeric heterochromatin of this specific telomere leads to telomere lengthening of only that telomere in *cis*, but not at other telomeres. Therefore, this work describes a mechanism for a how telomere-specific repeat tract length can be established. Further, our results will force the evaluation of telomere length away from a generalized view to a more telomere-specific consideration.

Main:

Telomeric repeat DNA and associated proteins are required for maintaining genome stability [1]. In general, telomeric DNA is composed of short, guanine-rich repeats that render its replication particularly challenging [2]. The so-called end-replication problem will lead to telomere shortening at every cell division [3-5], and replication fork difficulties can lead to abrupt losses of a large part of the repeats [2]. Eventually, depending on the initial set-length of the telomeric repeat tracts, telomeric DNA becomes too short to assume telomeric functions and cells enter a permanent cell cycle arrest called cellular senescence [6,7]. This telomere-length derived limitation of cell divisions on the one hand directly contributes to age-related degenerative disease, and on the other hand also restricts cells from undergoing uncontrolled cell divisions that may lead to cancer [8,9]. Therefore, telomere equilibrium set-length is a key parameter that will affect the timing of onset of senescence and needs to be strictly regulated for optimal organismal function.

This telomere set-length is thought to be determined very early in life. Young humans have a set-length of about 10-12 kb of telomeric repeats [10]. Currently, it is thought that very few, perhaps less than five, extremely short dysfunctional telomeres are sufficient to engage telomere-mediated cellular senescence [11-13]. If the cellular DNA-damage checkpoint machinery is compromised, senescence can be bypassed, and most cells die in replicative crisis [8,9]. However, some cells can pass crisis and advance to malignant transformation [8]. Given that it takes only few dysfunctional telomeres to initiate the events to senescence, it may very well matter which are the causative telomeres for the process.

We know very little about how the initial set-length for telomeric repeat DNA is determined. Furthermore, while it was shown that individual human [14,15] and yeast [16,17] telomeres can have telomere-specific set-lengths, the mechanism for how specific telomeres in the same cell could have significantly differing set-lengths remained unknown. Specifically, at least one yeast telomere, the telomere on chromosome IIIL (TEL03L), has a set-length that deviates dramatically from those of all other telomeres [16,18]. Our results here confirm that the telomere set-length of TEL03L is much longer than that of all the others. More significantly, we show that this is due to an extended spreading *in cis* of a heterochromatin-like domain. Specifically, an extended level of Sir4 at TEL03L is attracting telomerase via a Sir4-Yku80 interaction which links the TEL03L telomere to the telomerase RNA. This mechanism leads to an increased level of telomerase at telomere TEL03L and delineates how a telomere-specific

98 telomerase recruitment mode can affect the telomere set-length determination exclusively in
99 *cis*. Therefore, our results confirm telomere-specific telomere length regulation, and the work
100 overall defines the molecular mechanism for one telomere. Such mechanisms could
101 determine which telomeres have a higher or lower probability to be the first to become
102 dysfunctional, leading to the initiation of senescence.

103 In budding yeast, either of two types of subtelomeric sequences, called Y'- and X-
104 elements, occur directly adjacent to the terminal telomeric repeats [19]. Accordingly, telomeres
105 are classified as either X-telomeres or Y'-telomeres, each accounting for about half of all 32
106 telomeres in common lab-strains; 15 and 17 respectively in the strains used here. X-elements
107 are not highly conserved, but many have enough unique sequences to be distinguished for
108 single telomere analyses. During work on telomeric chromatin of such individual X-telomeres
109 we found that the telomeric repeat tract on the X-telomere 3L consistently was much longer
110 (510 ± 55 bp) than the previously described average of 300 ± 75 bp [19] (Fig. 1; Extended Fig.
111 1). This unexpected length for TEL03L was determined via TeloPCR (see Methods for details;
112 Fig. 1a, b) or by standard Southern blotting of genomic DNA digested with an appropriate
113 restriction enzyme (PvuII, Fig. 1c). DNA from the same WT strains analyzed using the more
114 common XhoI restriction digest and Southern blotting using a telomeric repeat probe did yield
115 the canonical expected sizes for Y'-telomeres (Extended Fig. 1a, c). Moreover, we also
116 performed pan-telomere analysis by chromosome end-to-end sequencing using nanopore
117 sequencing [17]. When we plotted the individual telomeric tract lengths for each telomere and
118 compared it to the average size of all telomeres, it became very evident that TEL03L was
119 significantly longer than any of the other telomeres (Fig. 1d). The fact that TEL03L is
120 exceptionally long had been reported when this telomere was first cloned [16], and more recent
121 data show that this also occurs in many yeast strains from around the globe, including all lab
122 strains [18].

123 We thus wished to investigate how this very long equilibrium set-length at TEL03L was
124 established and maintained. Telomere maintenance can be dependent on homologous
125 recombination or on the telomerase enzyme [19]. Examining telomere lengths by Southern
126 blotting in strains lacking Rad52 and that can not maintain telomeres by recombination
127 showed that the set-lengths of TEL03L in were indistinguishable in WT vs *rad52Δ* strains
128 (Extended Fig. 1b, c). Therefore, we surmised that the TEL03L telomere was maintained by a
129 telomerase dependent mechanism. In this case, the steady-state telomere length will be

determined by an equilibrium between telomere shortening activities and telomerase-mediated telomere lengthening activities. To examine whether the length of TEL03L was due to less shortening activities, we compared the loss rates at various telomeres to that at TEL03L in the absence of telomerase. Previous data showed that in strains lacking an essential telomerase component, telomeres lose approximately 3-5 bp/generation [17,20,21]. Given that we wanted to examine those losses immediately after telomerase loss, we fused Est3 and Est1, essential protein components of telomerase [19], to the FKBP12-rapamycin-binding domain of human TOR1 (FRB-domain) in the Anchor Away system [22]. This setup allowed us by simple addition of rapamycin to rapidly deplete the nuclear Est3/Est1 and examine telomeric sequence losses thereafter (Fig. 2). At the start of the experiments, telomere lengths for Y'-telomeres as well as those for X-telomeres TEL11R and TEL06R were in the range of 300 ± 75 bp (Fig. 2a). However, TEL03L was much longer at approximately 480bp. We then induced Est3-FRB expulsion from the nucleus by addition of rapamycin and measured telomere length changes during the next ten days (corresponding to ~95 population doublings (Fig. 2b, c). At the end, telomere loss rates were calculated as a function of population doublings for each X-telomere separately and the Y'-telomeres collectively (Fig. 2d; Extended Fig. 2a). Although there is some variability in the data, the sequence loss rates at TEL03L were not significantly lower than those for the other telomeres analyzed in either the Est3-FRB or the Est1-FRB experiments. This result is consistent with previous results indicating that upon loss of telomerase, overall similar sequence loss rates are observed, irrespective of the starting telomere length [17,23]. It also strongly suggests that it is the lengthening aspect of telomerase-dependent length maintenance that is more efficient at TEL03L.

The very long telomeric tracts on TEL03L occur in many yeast strain backgrounds, including wild yeast strains collected in nature [18]. Furthermore, the sequences on TEL03L, including the terminal repeats themselves, are highly conserved between strains. Therefore, the terminal sequence of TEL03L itself might have been at the base of the telomere-specific long set-length. We considered that either the TEL03L X-element or some special terminal repeat arrangement caused the long set-length. To examine those two possibilities, we replaced the terminal TEL03L X-element with the X-element present on TEL01L ending with a short telomeric seed sequence (see Extended Fig. 2b for details). As a control to examine the terminal repeat sequences only, the replacement procedure was also performed with the

original TEL03L X-element that harbored only a short telomeric repeat seed, followed by assessing the regrowth of the TEL03L in this situation (see Extended Fig. 2b). Remarkably, both situations allowed for a lengthening of the modified TEL03L to well beyond the average 300 bp size of telomeric repeat tracts in the cells: telomeric tract lengths as measured by Southern blotting were 420±40 bp for TEL03L-3L and 451±56 bp for TEL03L-1L (Fig. 3a, b; Extended Fig. 3a). Similar results were obtained when the altered TEL03Ls were analyzed by TeloPCR (Extended Fig. 3b). The TEL03L wt before modification was at 466±65 bp. These data therefore show that the long set-length of TEL03L is not due to a special TEL03L X-element or a particular terminal repeat arrangement.

A unique feature of budding yeast chromosome III is the fact that it contains near its centromere a locus that determines haploid mating behavior (*MATa* or *MATα*). In addition, there are silenced copies of those mating type specifying genes near the telomeres of chromosome III: *HMR*, about 20 kb from telomere TEL03R [24]; and *HML* about 10 kb from TEL03L [16]. Silencing of those *HM*-loci depends on the association of a set of Sir-proteins (Sir1, Sir2, Sir3 and Sir4) [25]. In fact, transcriptional silencing can also be observed near telomeres [26], and this repression is dependent on the Sir2, Sir3 and Sir4 proteins, but not on Sir1 [27]. As part of the investigations on sequence determinants of TEL03L overextension, we deleted *HML* or *HMR* from the genome and discovered that deletion of *HML*, but not *HMR*, partly suppressed the long set-length phenotype on TEL03L (Fig. 3c, d; Extended Fig. 3a). These deletions did not affect telomeric repeat lengths of X-telomeres TEL11L, TEL06R or TEL11R (Extended Fig. 3c, 3d). The overall length of all 17 Y'-telomeres is not affected by these deletions either (Extended Fig. 3d). Given this result, we investigated whether the Sir-proteins would affect TEL03L set-length. Indeed, deletion of any of the *SIR2, SIR3* or *SIR4* genes shortened the long telomere phenotype of TEL03L such that the set-length of this telomere now became indistinguishable from the median of all telomeres in the cell (Figure 4a, b; Extended Fig. 1a; Extended Fig. 4a). As reported previously [28], we also noticed that the deletion of the *SIR4* gene caused a slight reduction in the size of all telomeres, and remarkably, TEL03L also further adjusted to the slightly shorter overall lengths (Figure 4a, b; Extended Fig. 1a). Specifically, the average telomere length in a *sir2*Δ strain measured 342±20 bp and that of TEL03L matched that size quite well 312±10 bp; in a *sir4*Δ strain, overall lengths were reduced to 276±21 bp and that of TEL03L to 256±14 bp (Figure 4a, b; Extended Fig. 1a; Extended Fig. 4a). Remarkably, in a *sir1*Δ strain, the overall telomere set-

lengths were not significantly affected (372±10 bp), but the length of TEL03L was reduced from around 559±87 bp to 487±30 bp (Fig. 4a); the latter being similar to the size measured for this telomere in the *hml*Δ strain (487±78, Fig. 3c, d). A similar shortening of TEL03L from the extended set-length length in wt cells to the more canonical 300 bp in a *sir3*Δ strain was also documented with the nano-pore sequencing method (Extended Fig. 4b).

Telomerase recruitment in yeast depends on an essential interaction between the Est1 component on telomerase and the telomere-bound Cdc13 protein [19]. However, the yeast yKu heterodimer, composed of Yku70/Yku80, also interacts with the telomerase RNA, Tlc1 [29]. Furthermore, Yku80 interacts with Sir4, which in turn can interact with the telomere-bound Rap1 protein. This Tlc1-Yku70/Yku80-Sir4 axis provides for accessory telomerase recruitment lengthening telomeres by about 50 bp [30,31]. Given the above, we hypothesized that the long set-length on TEL03L may be due to this recruitment mode. This idea predicts that in strains harboring any mutations that disrupt this axis, all telomeres would be equally dependent on the Est1-Cdc13 recruitment and have the same set-lengths. We therefore introduced alleles that interrupt the axis and compared global telomere set-length to the one on TEL03L. The telomerase RNA allele *tlc1-Δ48* does not interact with yeast yKu [29] and the *yku80-L140A* allele of *YKU80* can not interact with Sir4 [32]. The average telomere lengths decreased slightly in strains with the *tlc1-Δ48*, *yku80-L140A* or the *sir4*Δ alleles (Fig. 5a, b; Extended Fig 5), consistent with previous data [29,32]. Remarkably, in all three strains, the set-length of TEL03L was reduced to the same lengths as the mean of all telomeres (Fig. 5b, Extended Fig 5a, b, c). These results thus show that the long telomere set-length of TEL03L is dependent on the Tlc1-Tku70/Yku80-Sir4 telomerase recruitment axis, which would mediate telomere-specific levels of telomere-telomerase interactions. Consistent with the above, there is evidence that on TEL03L, the Sir2/3/4-proteins spread from the distal telomeric X-element and are associated with the entire 10 kb sequence between the *HML* locus and TEL03L [33,34]. This can explain the significantly increased presence of Sir4 on this telomeric locus. On virtually all other natural telomeres, the Sir-complex does not spread much beyond the telomeric repeat DNA on Y'-telomeres, or beyond the proximal end of the X-elements [33,34]. It is therefore thought that except for the proximal end of the X-element on TEL03L, there is a strong chromatin boundary at these transition sites [33-35]. However, given that the telomeric repeat tract distal of the X-element of TEL01L also becomes very long if that X-element is placed

onto the end of telomere 3L (Fig. 3), we hypothesized that Sir-protein coverage from TEL03L to the *HML* locus may be due to a locus-specific weakening of boundary elements.

If indeed a weakened boundary element at TEL03L was the reason for Sir2/3/4 spreading and causing the long set-length on TEL03L, mutations in boundary element proteins, such as Tbf1 [35], may weaken the boundary effect in general, allowing more spreading of Sir4 on all telomeres and leading to overall telomere lengthening. Boundary element proteins such as Tbf1, Reb1, or Abf1 are also important general transcription factors and essential in yeast [19]. Therefore, we screened for a new allele of *TBF1* that still supports cell viability but in which the boundary function is reduced. The *tbf1-453* allele fulfills these requirements and contains a single amino acid change (Q453H). Cells with this allele grow slowly but are viable at 30°C, and they do not exhibit any major change in their transcriptomic profiles (Extended Fig. 6a, b, c). Moreover, in cells with the *tbf1-453* allele, the abundance of the Sir4 protein significantly increases on telomere adjacent sites (1.5 kb to 3.1 kb from the transition of subtelomeric to the respective X-elements; Extended Fig. 6d). Finally, in these cells, all analyzed telomeres are hyper-elongating, including X-telomeres TEL06R, TEL11L, TEL11R, TEL03L, and the Y'-telomeres (Fig. 6; Extended Fig. 7). Moreover, this telomere lengthening is specific to the *tbf1-453* allele and not observed in cells lacking another telomeric chromatin associated protein such as Rpd3 (Extended Fig. 7). Deleting any of the *SIR2, SIR3 or SIR4* genes in cells with the *tbf1-453* allele however is epistatic and reduces the elongated set length of the telomeres (Fig. 6), as predicted if the over elongation of telomeres in the *tbf1-453* cells is dependent on Sir-protein spreading.

To verify whether two closely positioned sites with active Sir-protein binding are sufficient to cause Sir4 spreading in between them, we moved the entire *HML* locus onto two other X-telomeres (TEL01L and TEL15L) at less than 10 kb from the very end. In both cases the repeat tract on the control TEL03L remained at its very long equilibrium length (500 ± 24 bp and 460 ± 24 bp respectively, Suppl. Figs. 1, 2). The specific telomeres with the added *HML* locus however did not lengthen (Suppl. Fig. 1b, 2b). Sir-protein binding at the transposed *HML* loci appeared to occur normally since these MATa strains mated efficiently to MATα strains (Suppl. Fig. 3), a process that is impaired, if the *HML* locus is de-repressed (see the MATa *sir3*Δ strain in Suppl. Fig. 3a). Finally, we also engineered a strain in which the *HMR* locus is closer than 10 kb from the telomeric end on TEL03R, yet again, this TEL03R variant did not display a long set-length phenotype (Suppl. Fig. 4). Therefore, there must be a

locus specific effect on TEL03L that allows for Sir-protein occupation between the *HML* locus and the TEL03L telomere.

The analyses presented here show that on TEL03L in yeast, an extended binding of Sir4 on the terminal 10 kb of DNA is responsible for a very long equilibrium set-length of telomeric repeats specifically at this telomere. Indeed, the Sir2/3/4-proteins have been shown to be associated with the terminal 10 kb sequence on TEL03L between *HML* and the telomeric repeats [33,34]. It is well established that the Sir-proteins associate with regions requiring transcriptional silencing, such as the *HML* and *HMR* loci [25]. In addition, the Sir2/3/4-proteins, but not Sir1, also strongly associate with telomeres and subtelomeric X-elements [33,34]. However, on all native telomeres except TEL03L, centromere proximal from the X-elements there is only very limited presence of the Sir2/3/4-proteins [33,34]. The abrupt loss of Sir-association at the centromere proximal side of the X-elements or at the transitions between telomeric repeat DNA and the Y'-element closely parallels the loss of transcriptional repression in native telomere environments, an effect ascribed to boundary elements at these transition sites [35,36]. Our data show that in an experimental setting with generally increased Sir4-spreading; in cells with the *tbf1-453* allele, all analyzed telomeres, including TEL03L, lengthen to a new set-length that is approximately 50 bp longer than in WT (Fig. 6; Extended Fig. 7).

Next, our data show that the very long set-telomere length on TEL03L is dependent on the yKu-Sir4 protein interaction that bridges Sir4-bound telomeric loci to yKu-bound telomerase RNA (Figs. 4, 5). It was reported before that for Y-telomeres, this non-essential telomerase recruitment mode results in a 50 bp increase of the telomere set-length from about 260 bp, in the absence of the yKu-Sir4 axis, to about 300 bp in WT cells [28,29] Fig. 4, 5). However, on TEL03L, the set-length is increased from 260 bp to ≥ 500 bp (Fig. 1) in a telomerase-dependent manner (Fig. 2). The X-element on TEL03L is not required for the long set-length on TEL03L, because replacing this 03L-X with the one of TEL01L (01L-X) also results in a very long set-length on TEL03L. By extension, the boundary element on the TEL03L-X does not appear to differ from other boundary elements. Interestingly, the presence of the *HML* locus does affect the set-length of TEL03L by a significant amount (Fig. 3, 5, Extended Fig. 3), but has no effect on the set-lengths of other telomeres. We ascribe this result to the strong association of the Sir-complex with the *HML* locus. Consistent with this idea, the fully elongated set-length at TEL03L is dependent on the Sir1 protein and the

289 presence of the *HML* locus, but the equilibrium set-lengths of other telomeres are not
290 significantly influenced by their presence or absence (Fig. 4; Extended Fig. 1, [27]). These
291 results therefore detail the molecular requirements for how the very long set-length of TEL03L
292 is achieved: an increased association of the Sir4 protein over 10 kb of telomere-adjacent
293 chromatin yields increased Sir4-yKu mediated telomere-telomerase interactions. The latter
294 allows for increased telomere elongation events in *cis* on this telomere, leading to a long set-
295 length telomere. This mechanism also explains why tethering of the Sir4 protein to a specific
296 telomere will cause lengthening exclusively of that particular telomere [37]. We attempted to
297 transpose these elements for a long set-length onto other telomeres by inserting the *HML*
298 locus at less than 10 kb from the distal end of X-telomeres TEL01L or TEL15L, but the set
299 length of those artificially constructed ends did not change (Suppl. Figs. 1-3). Similarly, we
300 altered TEL03R in such a way that the *HMR* locus was less than 10 kb away from the
301 telomere, but that did not change the set-length of that telomere either (Suppl. Fig. 4).
302 Therefore, the Sir4 association between the TEL03L and the *HML* locus requires some locus-
303 specific feature of TEL03L that we have not identified yet and that there may be additional
304 mechanisms that regulate end-specific equilibrium telomere lengths.
305 Taken together, our results document one mechanism for how the equilibrium set-length
306 of telomeric repeats can be determined by subtelomeric chromatin in *cis* and thus lead to a
307 telomere-specific length homeostasis. Recent data indicates that in human cells, telomeres
308 also have chromosome end-specific set lengths [14,15]. For humans, telomere length is a critical
309 and limiting parameter for the number of cell divisions that can occur. For example, very short
310 telomeres lose their full capping function and are sensed by a telomere-specific DNA damage
311 response that induces cellular senescence [6,38]. Moreover, inappropriate telomere lengths are
312 associated with cancer development. Chromosome end-specific length differences predict
313 distinct telomeres may be the first to be sensed as dysfunctional, which will have important
314 implications for aging and cancer.
315

METHODS

Strains and plasmids

All strains are derivatives of W3749 *MATa*, a *RAD5*-corrected W303 strain [39] unless otherwise noted. The genotypes of the strains used in this study are described in Supplementary Table 1.

To delete Sir genes, we constructed GTy11, 12, and 13. These strains were obtained by a one-step replacement of the *SIR1, SIR2* and *SIR3* genes with a KanMX6 cassette. To delete *RAD52* we constructed JNy301 and JNy302 by a one-step replacement of *RAD52* with a *LEU2* cassette in W303 *MATa* and *MATα* [40].

For the anchor away system we constructed AHy001 and AHy005 strains from KLy18 strain by C-terminal tagging of *EST1* and *EST3* genes respectively by one-step PCR-mediated technique. The FRB::KanMX6 cassettes used for C-terminal tagging of Est1 and Est3 were obtained from amplification of pLK2 plasmid with primers Est1_CterTag_F and Est1_CterTag_R and Est3_CterTag_F and Est3_CterTag_R (Supplementary Table 2).

For the TEL03L X-element swap we constructed GTy26 and GTy27. GTy26 was constructed by transforming W303 *MATa* [40] with a plasmid containing TEL03L subtelomeric region, Tel03L x-element and telomeric repeats with a *LEU2* flanked by RS site (T3TD plasmid digested with NsiI/Eco53kI). After, the *LEU2* selection marker was recombined out obtaining the final strain. GTy27 was constructed by transforming W303 *MATa* WT with a plasmid containing TEL03L subtelomeric region, TEL01L X-element and telomeric repeats with a *LEU2* flanked by RS sites (pAH01 digested with NsiI/Eco53kI) that was recombined out to obtain the final strain.

For the deletion of *HML* and *HMR* loci, we constructed GTy02, GTy19 and 20. GTy02 was obtained by transformation of W3749A with pJH2039 [41] digested with HindIII-HF. GTy19 and 20 were obtained by transformation of W3749A with PCR fragments (primers Hml-F and R and Hmr-F and R (Supplementary Table 2) from plasmids pGT02 and pGT03 respectively.

For the deletion of the Ku stem of Tlc1 in W3749A strain we constructed GTy10. Plasmid pRS306-tlc1Δ48 digested with BsrGI was used for the integration and then, PCR was used to select correct recombination. For expression of Yku80 and Yku80-L140A, EPY129 strain was

transformed with the pJP7c plasmid (*YKU80-Mycx2-Hisx10*, CEN, *TRP1*) and pJP7C-L140A [42].

To construct *tbf-453* (ELy268-6b), site-directed mutagenesis primers (Supplementary Table 2) were designed to introduce the desired amino acid substitution into the pRS304-TBF1::NatMX plasmid which was then digested to obtain the desired fragment for integrating *tbf1-453* allele in the TBF1 locus to create a heterozygous diploid. Then, the strain was microdissected to obtain haploid strains. CLy05, CLy06 and GTy28 were obtained by a one-step replacement of the *SIR2, SIR3* and *SIR4* genes with a KanMX6 cassette in tbf1-453 strains. Strain GTy31 was obtained by a one-step replacement of the *RPD3* gene with a *TRP1* cassette.

To add HML to TEL01L and to TEL15L we constructed LBy126 and LBy129. In LBy126 HML was added 9912 bp away from the telomeric repeats of TEL01L (transformation of W3749A with pLB049 digested with MfeI-HF/SalI-HF). In LB129 HML was added 5289 bp away from the telomeric repeats of TEL15L (transformation of W3749A with pLB052 with NruI-HF and SalI-HF). For the deletion of 10 kb between HMR and TEL03R we constructed GTY29 and GTY30. GTY29 was obtained by transformation of W3749A with pGT05 digested with SalI and SacI. GTy30 is the replacement of the Y' of TEL03R for the X-element of TEL01L. It was obtained by transformation of W3749A with pGT06 digested with NotI and AflII. The *URA3* flanked by RS sites was recombined out to obtain the final strain.

Strains containing the *tbf1-453* and *sir4-myc* alleles were constructed by mating W3749 (*tbf1-453)* with a *SIR4-Myc* W303 (JC3433 W303 *MATa* with *SIR4-13Myc::KanMX*) [43]. Then strains were microdissected to obtain haploid strains.

Yeast strains obtained were verified by PCR followed by sequencing or Southern blot. In all experiments, yeast cells were grown at 30 °C with constant agitation in standard conditions (YEP or YC media with appropriate carbon sources).

Plasmids are described in Supplementary Table 3 and all plasmids used were verified by sequencing.

T3TD was obtained by Gibson Assembly to be able to insert the subtelomere of TEL03L, *LEU2* flanked by R-sites and the X-element of TEL03L into the NsiI-NotI sites of pRS303. Then, telomeric repeats were inserted into the NruI-NotI sites of the new plasmid.

pAH01 was obtained by replacing X-element of TEL03L with X-element of TEL01L in T3TD (NcoI-NotI sites).

pGT01 and pGT02 were constructed by Gibson assembly by adding HML or HMR flanking sequences with the *TRP1* marker to a pRS303 plasmid.

pLB049 and pLB052 were obtained by a double ligation strategy to add the HML, the *URA3* marker and flanking sequences of Chr1L (9912 bp away from TEL01L) and Chr15L (5289 bp away from TEL15L) to a pRS303 plasmid.

pGT05 was obtained by a double ligation strategy to delete 10 kb between HMR and TEL03R. Flanking sequences of Chr03R to be able to delete 10 kb and the *TRP1* marker were ligated to pRS303.

pGT06 was obtained by ligation strategy to be able to insert the subtelomere of TEL03R, *URA3* flanked by R-sites, the X-element of TEL01L and telomeric repeats into pRS303.

<u>DNA isolation and Southern blotting</u>

DNA was extracted using a standard phenol–chloroform procedure [44]. An appropriate quantity of digested DNA, ranging from 0.5 µg to 1 µg, was separated on 0.7% TBE (1 x) agarose gels, transferred onto a BrightStar™-Plus Positively Charged Nylon Membrane (Invitrogen) and hybridized to specific 32^{P}-labelled radioactive probes. Specific probes (TEL03L, TEL03R-1LX, TEL1L, TEL15L) to one chromosomal end were obtained by genomic DNA PCR-based amplification using specific primers followed by amplicon purification on gel and random priming labeling procedure [45]. Sequences of primers used to amplify a specific chromosomal end are depicted in Supplementary Table 2. As a telomeric repeat probe, a 300-bp fragment containing 280-bp TG repeats derived from pYLPV was radiolabelled using a random priming labeling procedure [46]. Data were visualized with a Typhoon FLA9000 apparatus. When necessary, membranes were stripped by boiling in 0.1% SDS and left at room temperature for 30 min and rehybridized with other radioactive probes. Data analysis GelAnalyzer software was used to determine the size of each detectable fragment.

TeloPCR

We modified the protocol based on Zubko *et al.* 2016 [47]. For the terminal transferase-mediated tailing of genomic DNA we used 60 ng of genomic DNA in a volume of 10 µL and the DNA was denatured at 95ºC for 5 min in a thermal cycler and cooled on ice. Then, 40 µL of transferase reaction mix was added to make total volume 50 µl. The transferase reaction mix contained 1X transferase buffer, 0.25 mM $CoCl_2$, 0.2 mM dCTP and 2 U of terminal transferase (New England Biolabs). The mix was incubated at 37ºC for 30 min, and then the enzyme was heat inactivated at 70ºC for 10 min at. After heat inactivation, the tailing reactions were used in PCR.

PCRs for amplification of chromosomal termini were performed on tailed DNA in 20 µL using GoTaq® Long PCR master Mix (Promega). PCR mix included 10 µL of GoTaq® Long PCR master Mix, 0.5 M of a sub telomeric specific region, 1 M of a G tail primer (Supplementary Table 2) and 1 µL of C-tailed genomic DNA. PCR conditions were the following:

95 ºC - 2 min, and then 40 cycles at 95 ºC - 20 s, 65 ºC - 30 s, 65 ºC - 2 min with final extension at 72 ºC for 10 min. PCR reactions were carried out in 0.2 mL tubes (VWR) using Bio Rad T-100 Thermal Cycler. After PCR a 1.2% TBE 0.5X gel was run overnight at 40 volts.

Nanopore sequencing

DNA molecular end tagging

High molecular weight genomic DNA extraction and DNA molecular end tagging of BY4741 WT [48] and BY4741 *sir3*Δ were done according to Sholes *et al*. 2021 [17]

Nanopore library preparation and sequencing

Library preparation of 1µg input DNA with a molecular tag was performed using the Native barcoding genomic DNA kit (Oxford Nanopore Technologies EXP-NBD104 and SQK-LSK109). Samples were run on a MinION flow cell (v.9.4.1) for 24 to 72 hours and were operated using the MinKNOW software (v.19.2.2). Only reads with barcodes on both ends were selected to pass.

Analysis of telomere length by nanopore sequencing

To analyze individual telomere length from nanopore sequencing, software has been developed and the code is hosted on GitHub (https://github.com/jflucier/E2EAssembler). The first step allows genome assembly from Nanopore sequencing data for each strain. We divided the sequencing reads into different parts, each with a total genome coverage of approximately 60X. We used Canu assembly software to individually assemble each different part. The produced assemblies were then merged [49]. The second step consists of the annotation of subtelomeres, telomeric repeats, and telotag on the assembled genome. The third step consists of the extraction of length value of telomeric tracts for each read from the different chromosome ends. Data representation was done using R software.

Anchor away system

We modified the protocol based on Haruki *et al*. 2008 [22]. Senescence assays of anchor-away strains have been performed with 2 WT clones, 3 independent clones of EST1-FRB and 3 clones of EST3-FRB. YEPD supplemented with rapamycin at 1 µg/ml final (YEPD + Rapamycin) was freshly made daily. After an overnight pre-culture in YEPD, cells were diluted at $0.04x10^7$ cells/ml in YEPD + Rapamycin. After 24 hours, OD_{660} was measured, and cells were diluted to $0.04x10^7$ cells/ml in YEPD + Rapamycin. Population doublings were calculated using OD_{660} measurements converted to cells/ml using a standardized chart. The process was repeated each day for 14 days and for each day, the remaining cells were pelleted, and DNA was extracted.

Assay of yeast mating reaction

To test if LBy126 and LBy129 could mate we used a qualitative strategy using auxotrophic markers that complement the nutritional requirements [50]. We used SGY401 as a MATα strain and EPY135: MATa *sir3Δ* as a non-mating strain control.

Chromatin immunoprecipitation and qPCR

Chromatin immunoprecipitation experiments were performed as previously described [51] with minor modifications. Briefly, 100mL cultures per ChIP were grown at 30 °C to OD_{600nm} 0.5–0.8. Cells were cross-linked with 1% formaldehyde for 10 min. After stopping the cross-link reaction and washes, cells were lysed in 500 µL ChIP lysis buffer (50 mM HEPES–KOH pH 7.5, 140 mM NaCl, 1 mM EDTA pH 8.0, 1% Triton X-100, 0.1% Na-deoxycholate, 1 mM PMSF) with glass beads using a FastPrep (MP Biomedicals). Following sonication, 500 µL of whole cell extract (WCE) was incubated overnight at 4°C with 2 µg anti-*c*-myc antibodies (mouse monoclonal, clone 9E10, Roche) for immunoprecipitation of myc-tagged proteins. The next day, 50 µL equilibrated Pierce protein A/G magnetic beads (Thermo Fisher Scientific) were added for a 2 hour incubation at 4 °C. The purified immunoprecipitated and input DNAs were diluted and subjected to qPCR using appropriate primers (Supplementary Table 2) and PerfeCTa SYBR Green SuperMix (Quantabio, 95054-02K).

The percent input method was used to analyze qPCR signals. Briefly, the input signal was adjusted to 100% using the formula: Ct Input - log2 of dilution factor. The ΔCq was calculated using: Ct IP - adjusted Ct input. The percent input was then calculated using the formula:

$$\% \text{ input} = 2^{-[Ct(IP)]-[Ct(input)-\log2(\text{dilution factor})]} \times 100$$

qPCR reactions were performed in technical triplicates for 3 independent biological cultures. The mean, standard deviation and statistics for independent biological replicates are reported.

Total RNA sequencing

For total RNA extractions, 10 mL of yeast cells were grown to approximately OD_{600} 0.8, washed, resuspended in 500 µL LETS buffer and lysed by glass beads. Samples were extracted twice with phenol/chloroform/isoamyl alcohol (25:24:1) and once with chloroform/isoamyl alcohol (24:1). RNA was precipitated with 30 µL 3M NaOAc and 1 ml cold 100% ethanol. Samples were washed with 70% EtOH, dried, and resuspended in 20 µL of

nuclease-free water and quantified. RNA integrity was assessed with an Agilent 2100 Bioanalyzer (Agilent Technologies). Libraries were quantified and subjected to RNA-sequencing by Illumina PE100bp Hiseq 4000.

Statistics and reproducibility

GraphPad prism was used to perform all statistical analyses. Statistical differences of mean values of measurements were determined by two-tailed unpaired Student t test. Significance was denoted as ns for not significant, $*$ for $p < 0.05$, $**$ for $p < 0.01$, $***$ for $p < 0.001$.

Data Availability

The dataset on the whole genome raw sequencing reads generated in this study has been submitted to the NCBI BioProject database under accession number PRJNA1088003. The Illumina RNA-seq data have been submitted to the NCBI BioProject database under accession number PRJNA1099244.

AUTHOR CONTRIBUTIONS

GMT and EP performed all biochemical and *in vivo* experiments; EB, EDL and LB contributed strain constructions, ChIP and RNA seq experiments; J-FL wrote scripts for nanopore sequencing analyses; SS and CWG supported and performed nanopore sequencing, RJW study conception, design and financing. RJW wrote and edited the manuscript with input of all co-authors.

ACKNOWLEDGEMENTS

We thank the Wellinger lab for constructive discussions and A. Krallis, A. Hewitt, and C. Levasseur for experimental help during the early phase of the project and with the anchor away experiments. We also thank the Brewer/Raghuraman lab for tools used in the anchor away system. Work for this manuscript was supported by a grant from the National Institutes for Health (NIH grant RO1GM152471) to CWG; a grant from the Canadian Institutes for Health Research (CIHR; foundation grant FDN154315); funds from the Canadian Research Chair on Telomere Biology to RJW; a post-doctoral fellowships to GMT from the Sherbrooke Center for Aging Research (CdRV); and a post-doctoral fellowship to LB from the Fonds de Recherche du Québec – Santé (FRQS).

CONFLICT OF INTEREST

The authors declare no conflict of interest.

524 **REFERENCES:**

525

526 1 de Lange, T. Shelterin-Mediated Telomere Protection. *Annu Rev Genet* **52**, 223-247
527 (2018). https://doi.org/10.1146/annurev-genet-032918-021921
528 2 Brenner, K. A. & Nandakumar, J. Consequences of telomere replication failure: the
529 other end-replication problem. *Trends Biochem Sci* **47**, 506-517 (2022).
530 https://doi.org/10.1016/j.tibs.2022.03.013
531 3 Hastie, N. D. *et al.* Telomere reduction in human colorectal carcinoma and with ageing.
532 *Nature* **346**, 866-868 (1990). https://doi.org/10.1038/346866a0
533 4 Harley, C. B., Futcher, A. B. & Greider, C. W. Telomeres shorten during ageing of
534 human fibroblasts. *Nature* **345**, 458-460 (1990).
535 5 Watson, J. D. Origin of concatemeric T7 DNA. *Nat New Biol* **239**, 197-201 (1972).
536 6 d'Adda di Fagagna, F. *et al.* A DNA damage checkpoint response in telomere-initiated
537 senescence. *Nature* **426**, 194-198 (2003).
538 7 Enomoto, S., Glowczewski, L. & Berman, J. MEC3, MEC1, and DDC2 are essential
539 components of a telomere checkpoint pathway required for cell cycle arrest during
540 senescence in Saccharomyces cerevisiae. *Mol Biol Cell* **13**, 2626-2638 (2002).
541 https://doi.org/10.1091/mbc.02-02-0012
542 8 Nassour, J., Schmidt, T. T. & Karlseder, J. Telomeres and Cancer: Resolving the
543 Paradox. *Annu Rev Cancer Biol* **5**, 59-77 (2021). https://doi.org/10.1146/annurev-
544 cancerbio-050420-023410
545 9 Cesare, A. J. & Karlseder, J. A three-state model of telomere control over human
546 proliferative boundaries. *Curr Opin Cell Biol* **24**, 731-738 (2012).
547 https://doi.org/10.1016/j.ceb.2012.08.007
548 10 Lansdorp, P. M. Telomeres, aging, and cancer: the big picture. *Blood* **139**, 813-821
549 (2022). https://doi.org/10.1182/blood.2021014299
550 11 Kaul, Z., Cesare, A. J., Huschtscha, L. I., Neumann, A. A. & Reddel, R. R. Five
551 dysfunctional telomeres predict onset of senescence in human cells. *EMBO Rep* **13**,
552 52-59 (2011). https://doi.org/10.1038/embor.2011.227
553 12 Khadaroo, B. *et al.* The DNA damage response at eroded telomeres and tethering to
554 the nuclear pore complex. *Nat Cell Biol* **11**, 980-987 (2009).
555 https://doi.org/10.1038/ncb1910
556 13 Abdallah, P. *et al.* A two-step model for senescence triggered by a single critically short
557 telomere. *Nat Cell Biol* **11**, 988-993 (2009). https://doi.org/10.1038/ncb1911
558 14 Karimian, K. *et al.* Human telomere length is chromosome end-specific and conserved
559 across individuals. *Science*, eado0431 (2024). https://doi.org/10.1126/science.ado0431
560 15 Martens, U. M. *et al.* Short telomeres on human chromosome 17p. *Nat Genet* **18**, 76-
561 80 (1998).
562 16 Button, L. L. & Astell, C. R. The Saccharomyces cerevisiae chromosome III left
563 telomere has a type X, but not a type Y', ARS region. *Mol Cell Biol* **6**, 1352-1356
564 (1986). https://doi.org/10.1128/mcb.6.4.1352-1356.1986
565 17 Sholes, S. L. *et al.* Chromosome-specific telomere lengths and the minimal functional
566 telomere revealed by nanopore sequencing. *Genome Res* **32**, 616-628 (2022).
567 https://doi.org/10.1101/gr.275868.121
568 18 O'Donnell, S. *et al.* Telomere-to-telomere assemblies of 142 strains characterize the
569 genome structural landscape in Saccharomyces cerevisiae. *Nat Genet* **55**, 1390-1399
570 (2023). https://doi.org/10.1038/s41588-023-01459-y

571 19 Wellinger, R. J. & Zakian, V. A. Everything you ever wanted to know about
572 Saccharomyces cerevisiae telomeres: beginning to end. *Genetics* **191**, 1073-1105
573 (2012). https://doi.org/10.1534/genetics.111.137851
574 20 Singer, M. S. & Gottschling, D. E. TLC1: template RNA component of Saccharomyces
575 cerevisiae telomerase. *Science* **266**, 404-409 (1994).
576 21 Soudet, J., Jolivet, P. & Teixeira, M. T. Elucidation of the DNA end-replication problem
577 in Saccharomyces cerevisiae. *Mol Cell* **53**, 954-964 (2014).
578 https://doi.org/10.1016/j.molcel.2014.02.030
579 22 Haruki, H., Nishikawa, J. & Laemmli, U. K. The anchor-away technique: rapid,
580 conditional establishment of yeast mutant phenotypes. *Mol Cell* **31**, 925-932 (2008).
581 https://doi.org/10.1016/j.molcel.2008.07.020
582 23 Marcand, S., Brevet, V. & Gilson, E. Progressive cis-inhibition of telomerase upon
583 telomere elongation. *Embo J* **18**, 3509-3519 (1999).
584 24 Oliver, S. G. *et al.* The complete DNA sequence of yeast chromosome III. *Nature* **357**,
585 38-46 (1992). https://doi.org/10.1038/357038a0
586 25 Rine, J. & Herskowitz, I. Four genes responsible for a position effect on expression
587 from HML and HMR in Saccharomyces cerevisiae. *Genetics* **116**, 9-22. (1987).
588 26 Gottschling, D. E., Aparicio, O. M., Billington, B. L. & Zakian, V. A. Position effect at S.
589 cerevisiae telomeres: reversible repression of Pol II transcription. *Cell* **63**, 751-762
590 (1990).
591 27 Aparicio, O. M., Billington, B. L. & Gottschling, D. E. Modifiers of position effect are
592 shared between telomeric and silent mating-type loci in S. cerevisiae. *Cell* **66**, 1279-
593 1287 (1991).
594 28 Palladino, F. *et al.* SIR3 and SIR4 proteins are required for the positioning and integrity
595 of yeast telomeres. *Cell* **75**, 543-555 (1993).
596 29 Peterson, S. E. *et al.* The function of a stem-loop in telomerase RNA is linked to the
597 DNA repair protein Ku. *Nat Genet* **27**, 64-67. (2001).
598 30 Roy, R., Meier, B., McAinsh, A. D., Feldmann, H. M. & Jackson, S. P. Separation-of-
599 function mutants of yeast Ku80 reveal a Yku80p-Sir4p interaction involved in telomeric
600 silencing. *J Biol Chem* **279**, 86-94 (2004).
601 31 Fisher, T. S., Taggart, A. K. P. & Zakian, V. A. Cell cycle-dependent regulation of yeast
602 telomerase by Ku. *Nature Structural & Molecular Biology* **11**, 1198-1205 (2004).
603 https://doi.org/10.1038/nsmb854
604 32 Ribes-Zamora, A., Mihalek, I., Lichtarge, O. & Bertuch, A. A. Distinct faces of the Ku
605 heterodimer mediate DNA repair and telomeric functions. *Nature Structural &*
606 *Molecular Biology* **14**, 301-307 (2007). https://doi.org/10.1038/nsmb1214
607 33 Radman-Livaja, M. *et al.* Dynamics of Sir3 spreading in budding yeast: secondary
608 recruitment sites and euchromatic localization. *EMBO J* **30**, 1012-1026 (2011).
609 https://doi.org/10.1038/emboj.2011.30
610 34 Brothers, M. & Rine, J. Distinguishing between recruitment and spread of silent
611 chromatin structures in Saccharomyces cerevisiae. *Elife* **11** (2022).
612 https://doi.org/10.7554/eLife.75653
613 35 Berthiau, A. S. *et al.* Subtelomeric proteins negatively regulate telomere elongation in
614 budding yeast. *Embo J* **25**, 846-856 (2006).
615 36 Pryde, F. E. & Louis, E. J. Limitations of silencing at native yeast telomeres. *Embo J*
616 **18**, 2538-2550 (1999).

37 Marcand, S., Gilson, E. & Shore, D. A protein-counting mechanism for telomere length regulation in yeast. *Science* **275**, 986-990 (1997). https://doi.org/10.1126/science.275.5302.986

38 Herbig, U., Jobling, W. A., Chen, B. P., Chen, D. J. & Sedivy, J. M. Telomere shortening triggers senescence of human cells through a pathway involving ATM, p53, and p21(CIP1), but not p16(INK4a). *Mol Cell* **14**, 501-513 (2004). https://doi.org/S1097276504002564 [pii]

39 Lisby, M. B., J. H.; Burgess, R. C.; Rothstein, R. . Choreography of the DNA damage response: spatiotemporal relationships among checkpoint and repair proteins. *Cell* **118**, 699-713 (2004). https://doi.org/10.1016/j.cell.2004.08.015

40 Thomas, B. J. R., R. Elevated recombination rates in transcriptionally active DNA. . *Cell* **56**, 619-630 (1989). https://doi.org/10.1016/0092-8674(89)90584-9

41 Li, J. *et al.* Regulation of budding yeast mating-type switching donor preference by the FHA domain of Fkh1. *PLoS Genet* **8**, e1002630 (2012). https://doi.org/10.1371/journal.pgen.1002630

42 Pfingsten, J. S. *et al.* Mutually exclusive binding of telomerase RNA and DNA by Ku alters telomerase recruitment model. *Cell* **148**, 922-932 (2012). https://doi.org/10.1016/j.cell.2012.01.033

43 Moradi-Fard, S. S., J.; Tittel-Elmer, M.; Lalonde, M.; Cusanelli, E.; Chartrand; P.; Cobb, J. A. . Smc5/6 Is a Telomere-Associated Complex that Regulates Sir4 Binding and TPE. *Plos Genet.* **12** (2016). https://doi.org/10.1371/journal.pgen.1006268.

44 Sambrook, J. F., E. F.; Maniatis, T. *Molecular cloning: a laboratory manual.*, Vol. 61 (Cold Spring Harbor Laboratory Press 1989).

45 Feinberg, A. P., ; Vogelstein, B. A technique for radiolabeling DNA restriction endonuclease fragments to high specific activity. . *Anal Biochem* **132**, 6-13 (1983). https://doi.org/10.1016/0003-2697(83)90418-9

46 Wellinger, R. J. W., A. J.; Zakian, V. A. . Saccharomyces telomeres acquire single-strand TG1-3 tails late in S phase. *Cell* **72**, 51-60 (1993). https://doi.org/10.1016/0092-8674(93)90049-v

47 Zubko, E. I. S., J.L.; Zubko, M. K. ATLAS: An advanced PCR-method for routine visualization of telomere length in Saccharomyces cerevisiae. *Int J Biol Macromol.* **93**, 1285-1294 (2016). https://doi.org/10.1016/j.ijbiomac.2016.09.006

48 Sikorski, R. S. & Hieter, P. A system of shuttle vectors and yeast host strains designed for efficient manipulation of DNA in Saccharomyces cerevisiae. *Genetics* **122**, 19-27 (1989). https://doi.org/10.1093/genetics/122.1.19

49 Wang, G. W., S.; Chai, X.; Zhang, J.; Yang, W.; Jiang, C.; Chen, K.; Miao, W.; Xiong, J. A strategy for complete telomere-to-telomere assembly of ciliate macronuclear genome using ultra-high coverage Nanopore data. . *Comput Struct Biotechnol J.* **19**, 1928-1932 (2021). https://doi.org/10.1016/j.csbj.2021.04.007.

50 Sprague, G. F. J. Assay of yeast mating reaction. *Methods Enzymol.* **194**, 77-93 (1991). https://doi.org/10.1016/0076-6879(91)94008-z

51 Pasquier, E. W., R. J. . In vivo chromatin organization on native yeast telomeric regions is independent of a cis-telomere loopback conformation. *Epigenetics Chromatin.* **13**, 23 (2020). https://doi.org/10.1186/s13072-020-00344-w

FIGURE LEGENDS:

Figure 1. Exceptionally long telomere set length on TEL03L

a TeloPCR analysis with DNA of 6 clones of WT W3749A. Telomeric DNA fragments amplified from TEL03L, TEL06R, and TEL11R. ***b***. Quantified telomeric tract lengths of the TeloPCR results in ***a*** (TEL03L, TEL06R and TEL11R; ∗∗∗ for $p < 0.001$, t-test). ***c*** Southern blot of DNA from 3 clones of WT W3749A digested with PvuII, hybridized with a radiolabeled telomeric repeat fragment. Telomeric bands TEL03L, TEL11L and TEL06R were sized and calculated tract lengths are indicated on right. ***d***. Telomere length distribution of each individual chromosome end from a BY4741 WT strain as obtained by Oxford Nanopore Sequencing. Straight vertical line indicates overall telomeric repeat average and the dashed line is the individual telomeric repeat length average of that particular telomere. Data for TEL04R is missing due to insufficient number of reads for this telomere.

Extended Figure 1. ***a***. Southern blot for telomeric fragments and plotted telomeric tract lengths on DNA derived from three clones each of W3749A WT, *sir1Δ* (GTY11), *sir2Δ* (GTY12), *sir3Δ* (GTY13) and *sir4Δ* (EPY031). DNA was digested with XhoI and hybridized with a telomeric repeat fragment. TEL06R and Y' tract lengths are indicated on right of blot. Quantitative statistics: ns for not significant and ∗∗∗ for $p < 0.001$, t-test. ***b***. Southern blot with DNA derived from three clones of W3749A, four clones of *rad52Δ MATa*, two clones of *rad52Δ MATα* and one clone of W3749α. DNA was digested with PvuII and probed with a telomeric repeat fragment. TEL03L, TEL11L and TEL06R telomeric repeat tract lengths are indicated on right. (ns for difference not significant, t-test). ***c***. 1. Table with TeloPCR results from Fig. 1*a*. Mean ± SD and p-value are detailed for TEL03L, TEL06R and TEL11R. 2. Table with Southern blot results from Fig. 1*b*. Mean ± SD and p-value are detailed for TEL03L, TEL11L and TEL06R. 3. Table with southern blot results from Extended Fig. 1*a*. Mean ± SD and p-value are detailed for TEL06R and Y'-telomeres. 4. Table with Southern blot results from Extended Fig. 1*b*. Mean ± SD and p-value are detailed for TEL03L, TEL11L, and TEL06R.

Figure 2. Comparable telomere shortening rates on all telomeres

a. Initial telomeric tract lengths for 3 clones of Est3-FRB are shown for TEL03L, TEL06R, TEL11R and Y'-telomeres. ***b***. Changing telomeric tract lengths of TEL11R, TEL06R and Y'-telomeres during culture outgrowth (14 days or indicated population doublings) of Est3-FRB cells. ***c***. Same as ***b*** but for TEL03L. ***d***. Calculated telomeric repeat loss rates (in bp/population doublings; bp/PDs) for Est1-FRB and Est3-FRB strains are tabled for TEL03L, TEL11R, TEL06R and Y'-telomeres. (ns for difference not significant, t-test).

Extended Figure 2. ***a***. 1 Table with initial telomeric tract lengths from Fig. 2a. Mean ± SD and p-value are detailed for TEL03L, TEL11R, TEL06R and Y'-telomeres. 2. All values for the loss rate analyses from Fig. 2d. Mean ± SD and p-value are detailed for TEL03L, TEL11R, TEL06R and Y'-telomeres. ***b***. Schematic drawing of the construction of strains GTY26 and GTY27. GTY26 was constructed with a DNA fragment containing a *LEU2* gene flanked by RS sites, the TEL03L X-element and a short seed of telomeric repeat. GTY27 was constructed with a DNA fragment containing a *LEU2* gene flanked by RS sites, the TEL01L X-element and a short seed of telomeric repeat. After loss of the *LEU2* marker gene by recombination, cells were grown for 100 generations. The positions of the HindIII restriction sites on TEL03L in strains GTY26, GTY27 and the WT are indicated.

Figure 3.

a. Southern blot and telomeric tract lengths of Tel03L-03L cells (GTY26), Tel03L-1L cells (GTY27) and WT cells with DNA digested with HindIII and probed with a TEL03L unique probe. ***b***. Quantified telomeric tract lengths (TEL03L) of the blot shown in ***a***. (ns for difference not significant, t-test). ***c***. Southern blot of DNA derived from W3749A WT cells, cells harboring *hmlΔ* (GTY19), and cells harboring *hmrΔ* (GTY20). DNA was digested with PvuII and probed with a TEL03L unique probe. ***d***. Quantified telomeric tract lengths (TEL03L) of the blot shown in ***c***. (∗ for $p < 0.05$ and ns for difference not significant, t-test).

Extended Figure 3. ***a***. 1. Table with Southern blot results from Fig. 3a. Mean ± SD and p-value are detailed for Tel03L. 2. Table with Southern blot results from Fig. 3c. Mean ± SD and p-value are detailed for TEL03L. ***b.*** TeloPCR of 3 clones of TEL03L-03L (GTY26) and 3 clones of TEL03L-1L (GTY27). Telomeric DNA fragments amplified from TEL03L. ***c.*** Southern

blot of 3 clones of W3749A WT, 3 clones of *hmlΔ* (GTY19), 3 clones of *hmrΔ* (GTY20) digested with PvuII and probed with a telomeric repeat fragment. ***d.*** Southern blot of 3 clones of W3749A WT, 3 clones of *hmlΔ* (GTY19), 3 clones of *hmrΔ* (GTY20) digested with XhoI and probed with a telomeric repeat fragment.

Figure 4: Long repeat tracts on TEL03L depend on the presence of Sir-proteins.
a. Southern blot of DNA derived from W3749A WT cells, *sir1Δ* (GTY11), of *sir2Δ* (GTY12), *sir3Δ* (GTY13) and *sir4Δ* (EPY031) cells, digested with PvuII and probed with a telomeric repeat fragment. ***b***. Quantified telomeric tract lengths from *a* of TEL03L, TEL11L and TEL06R are plotted with respect of the genotype (ns for difference not significant, $*$ for $p < 0.05$ and $***$ for $p < 0.001$, t-test).

Extended Figure 4. ***a.*** Table with Southern blot results from Fig. 4a. Mean ± SD and p-value are detailed for TEL03L, TEL11L, and TEL06R. ***b.*** Nanopore sequencing mapping of telomere length distributions of TEL03L and TEL06R in BY4741 WT versus BY4741 *sir3Δ* cells. Straight line indicates overall telomere length average of all telomeres and the dashed line is the individual telomere length average of that particular telomere.

Figure 5. Long repeat tracts on TEL03L are mediated by increased telomerase recruitment.
a. Left: Southern blot of DNA derived from W3749A WT cells, cells harboring the *tlc1Δ48* allele (GTY10), cells harboring the *hmlΔ* allele (GTY02), or cells with a *sir4Δ* allele (EPY031). DNA was digested with PvuII and hybridized to a telomeric repeat fragment. Right: Southern blot as on left, but with W3749A WT cells, cells with a *yku80Δ* allele (EPY129), EPY129 cells in which the *yku80Δ* allele is complemented by a plasmid-borne WT *YKU80* (indicated as p*YKU80*; strain GTY23) and EPY129 cells in which the *yku80Δ* allele is complemented by a plasmid-borne *yku80-L140A* allele (indicated as p*yku80-L140A*; strain GTY24). Bands labeled with an * are new recombinant X-telomere bands, but not TEL03L (see Extended Fig. 5a). ***b.*** Quantified telomeric tract lengths of TEL03L, TEL11L, TEL06R, and Y'-telomeres are plotted on the graph vs the indicated genotypes (ns for not significant, $*$ for $p < 0.05$, t-test). Southern blots for the data are in Fig. 5a, Extended Fig. 5a, b)

Extended Figure 5. ***a***. Southern blot of DNA from W3749A WT cells, cells with the *tlc1Δ48* allele (GTY10), cells with the *hmlΔ* allele (GTY02) and cells with the *sir4Δ* allele (EPY031). DNA was digested with PvuII and probed with a TEL03L unique probe. ***b***. Left: Southern blot with the same DNA as in Fig. 5a but digested with XhoI and probed with a telomeric repeat fragment. Right: DNA of cells of the indicated genotypes as in Fig. 5a but digested with XhoI and probed with a telomeric repeat fragment. ***c.*** All telomeric repeat tract quantifications with calculated means of at least three independent clones each, standard deviations, and significance calculations for the gels in Fig. 5 and Extended Fig. 5.

Figure 6. A boundary element mutation causes Sir4 spreading and telomere elongation. ***a*** Southern blot of DNA from W3749A WT cells, cells with the *tbf1-453* allele (ELY268-6b), cells with both the *tbf1- 453 and sir2Δ* alleles (CLY05), cells with both the *tbf1-453 and sir3Δ* alleles (CLY06), cells with both the *tbf1-453 and sir4Δ* alleles (GTY28). DNAs were digested with PvuII and probed with a telomeric repeat fragment. ***b.*** The telomeric tract lengths of TEL03L, TEL11L andTEL06R from the gel in *a* were quantified and plotted on the graph vs the indicated genotype (ns for not significant, $*$ for $p < 0.05$ and $**$ for $p < 0.01$, t-test).

Extended Figure 6. ***a.*** Detail of the single amino acid mutation in *tbf1-453* allele. ***b.*** Growth characteristics of cells with the *tbf1-453* allele vs WT. The four strains were derived from a microdissected heterozygous diploid strain. ***c.*** Selected results of mRNA seq analysis of total RNA derived from WT and *tbf1-453* cells. log2 ratios of the indicated genes are listed (See Data Availability section for access to all data). (+) indicates that the promoter of that gene contains a predicted Tbf1 binding site; (-) indicates that this gene does not contain such a site. ***d.*** Quantitative ChIP-PCR for Sir4 binding in telomere proximal areas of the indicated telomeres. Results from the procedure with untagged Sir4 or on the *MET3* locus served as negative controls (-); the *HMRa* locus (+) serves as a positive control. Primers are on the indicated telomeres at a distance from the X-element as indicated in brackets in kb. The differences between *TBF1* WT and *tbf1-453* on the indicated loci are significant with ** $p < 0.01$; t-test. For the other loci (not indicated) $p < 0.05$; t-test.

Extended Figure 7 a. Southern blot of DNA from W3749A WT cells, cells with the *rpd3Δ* allele (GTY31), cells with the *tbf1-453* allele (ELY268-6b), and cells with the *sir4Δ* allele (EPY031). The DNA was digested with XhoI (left part), or PvuII (right part) and hybridized to a telomeric repeat fragment. ***b.*** The quantified telomeric tract lengths of TEL03L, TEL11L and TEL06R vs the indicated genotypes are plotted (∗ for $p < 0.05$, ∗∗ for $p < 0.01$ and ∗∗∗ for $p < 0.001$, t-test). ***c.*** All telomeric repeat tract quantifications with calculated means of at least three independent clones each, standard deviations, and significance calculations for the gels in Fig. 6 and Extended Fig. 7.

Figure 1

a

Telo PCR (6 clones of W3749A each); Telomeres:

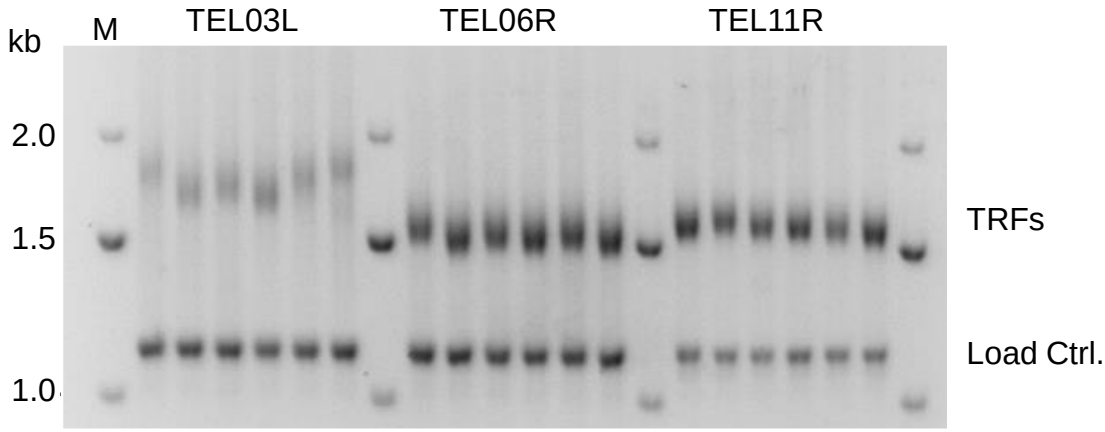

b

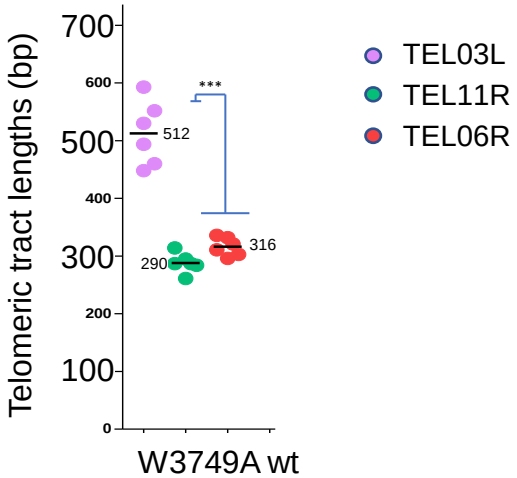

c

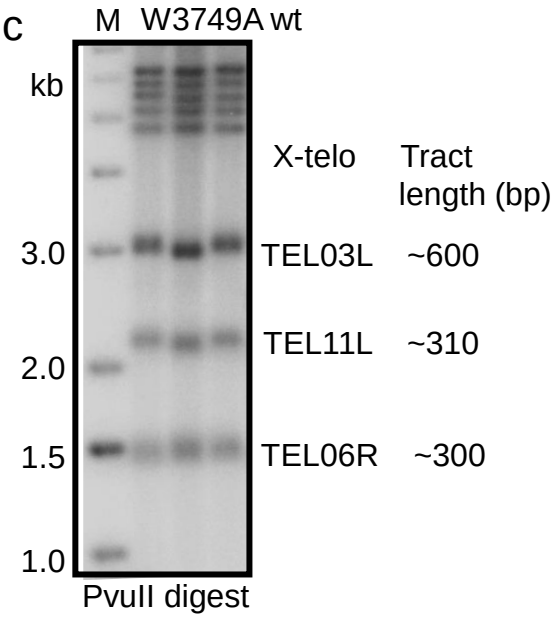

d

BY4741 WT

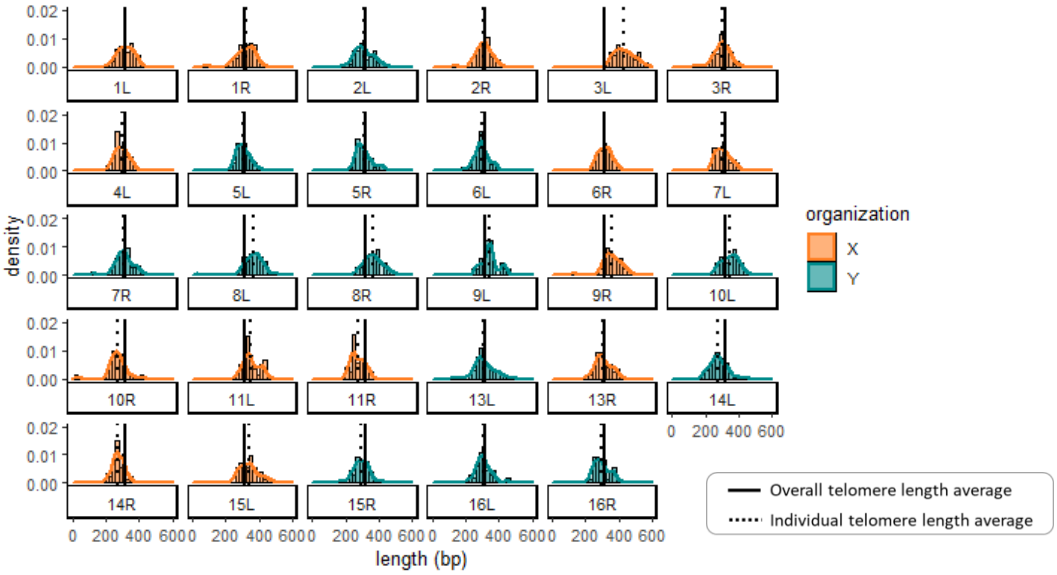

Extended Figure 1

a

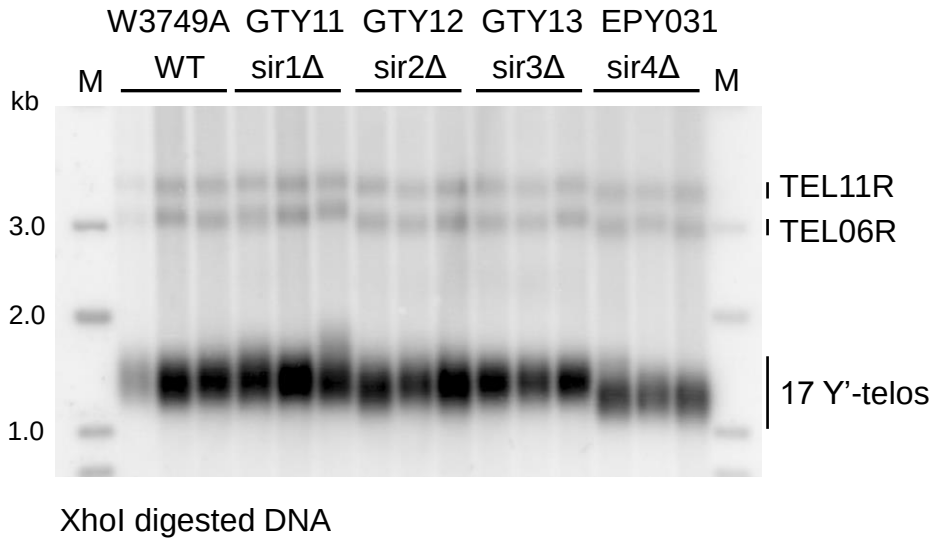

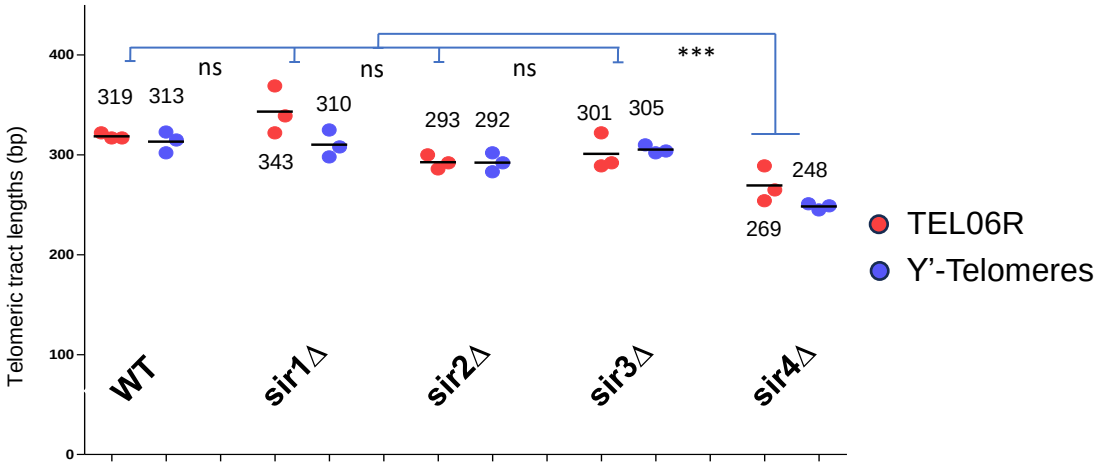

b

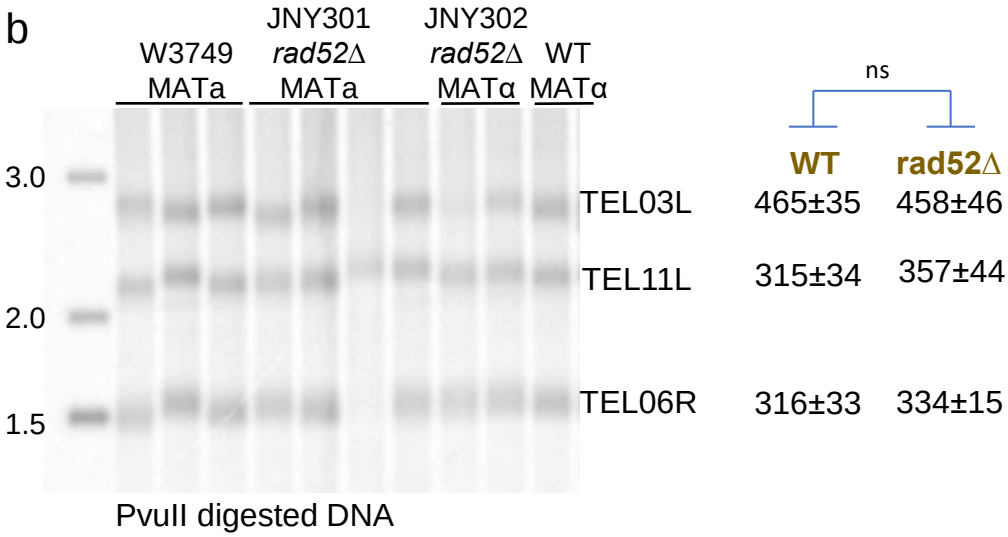

Extended Figure 1, continued

C

1

TeloPCR					
Genotype	**Telomere**	**Mean +/- SD**	**n**	**Difference with TEL03L**	
				Mean difference	**P-value**
W3749A	**TEL03L**	512.83 +/- 55.86	6		
W3749A	**TEL11R**	288 +/- 17.16	6	-224.83	< 0.0001***
W3749A	**TEL06R**	316.5 +/-15.95	6	-196.33	< 0.0001***

2

Blot					
Genotype	**Telomere**	**Mean +/- SD**	**n**	**Difference with TEL03L**	
				Mean difference	**P-value**
W3749A	**TEL03L**	745 +/- 26.88	3		
W3749A	**TEL11R**	328.33 +/- 56.21	3	-416,67	0.0003***
W3749A	**TEL06R**	309.33 +/- 8.08	3	-435,67	< 0.0001***

3

Blot (XhoI)					
Telomere	**Genotype**	**Mean ± SD**	**n**	**Difference with WT strain**	
				Mean difference	**P-value**
TEL06R	**W3749A (WT)**	318.66 ± 2.88	3		
TEL06R	***sir1Δ***	343.33 ± 23.79	3	24.67	0.1493
TEL06R	***sir2Δ***	292.66 ± 7.02	3	-26	0.0041
TEL06R	***sir3Δ***	301 ± 18.24	3	-17.66	0.173
TEL06R	***sir4Δ***	269.33 ± 17.89	3	-49.33	0.0092***
Y'	**W3749A (WT)**	313.33 ± 10.59	3		
Y'	***sir1Δ***	310.33 ± 13.65	3	-3	0.7786
Y'	***sir2Δ***	292.33 ± 9.50	3	-21	0.063
Y'	***sir3Δ***	305.33 ± 4.16	3	-8	0.2905
Y'	***sir4Δ***	248.33 ± 3.05	3	-65	0.0005***

4

Blot (PvuII)					
Telomere	**Genotype**	**Mean ± SD**	**n**	**Difference with WT strain**	
				Mean difference	**P-value**
TEL03L	W3749A (WT, *MAT*a)	465.33 ± 34.15	3		
TEL03L	*rad52Δ (MATa)*	458.33 ± 45.79	4	7	0.84
TEL03L	*rad52Δ (MATα)*	512 ± 24.04	2	-33.5	0.2
TEL03L	W3749α (WT, *MAT*α)	478.5 ± 7.77	2		
TEL11L	W3749A (WT, *MAT*a)	315 ± 34.07	3		
TEL11L	*rad52Δ (MATa)*	357 ± 44.39	4	-42	0.26
TEL11L	*rad52Δ (MATα)*	376.5 ± 19.09	2	-9	0.59
TEL11L	W3749α (WT, *MAT*α)	367.5 ± 6.36	2		
TEL06R	W3749A (WT, *MAT*a)	316 ± 33.05	3		
TEL06R	*rad52Δ (MATa)*	334 ± 15.10	4	-18	0.43
TEL06R	*rad52Δ (MATα)*	354.5 ± 0.70	2	-3	0.05
TEL06R	W3749α (WT, *MAT*α)	351.5 ± 0.70	2		

Figure 2

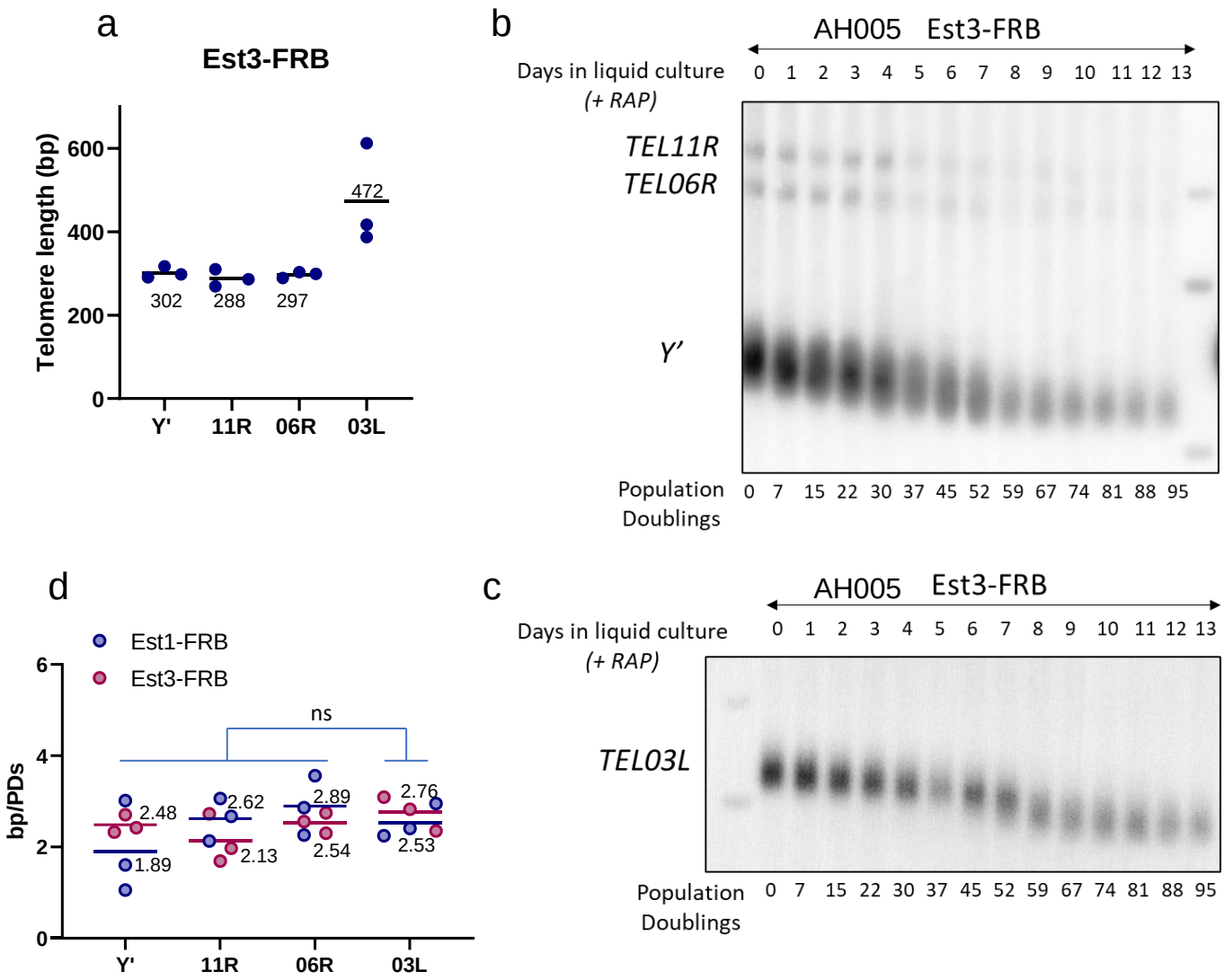
a
Est3-FRB
Telomere length (bp)
600
400
200
0
302
288
297
472
Y'
11R
06R
03L
b
AH005 Est3-FRB
Days in liquid culture
(+ RAP)
0 1 2 3 4 5 6 7 8 9 10 11 12 13
TEL11R
TEL06R
Y'
Population Doublings
0 7 15 22 30 37 45 52 59 67 74 81 88 95
d
Est1-FRB
Est3-FRB
bp/PDs
6
4
2
0
ns
2.48
1.89
2.62
2.13
2.89
2.54
2.76
2.53
Y'
11R
06R
03L
c
AH005 Est3-FRB
Days in liquid culture
(+ RAP)
0 1 2 3 4 5 6 7 8 9 10 11 12 13
TEL03L
Population Doublings
0 7 15 22 30 37 45 52 59 67 74 81 88 95

Extended Figure 2

a

1

Telomere length					
Genotype	Telomere	Mean +/- SD	n	Difference with TEL03L	
				Mean difference	P-value
EST3-FRB	TEL03L	472 ± 122.16	3		
EST3-FRB	TEL11R	288.33 ± 20.59	3	-183.67	0.0621
EST3-FRB	TEL06R	297 ± 7.21	3	-175	0.0684
EST3-FRB	Y'	302 ± 13.45	3	-170	0.0747

2

Population doubling					
Genotype	Telomere	Mean ± SD	n	Difference with TEL03L	
				Mean difference	P-value
EST1-FRB	TEL03L	2.53 ± 2.63	3		
EST1-FRB	TEL11R	2.62 ± 0.46	3		
EST1-FRB	TEL06R	2.89 ± 0.65	3		
EST1-FRB	Y'	1.89 ± 1.009	3		
EST3-FRB	TEL03L	2.75 ± 0.37	3		
EST3-FRB	TEL11R	2.12 ± 0.53	3	-0.63	0.31
EST3-FRB	TEL06R	2.53 ± 0.22	3	-0.22	0.7826
EST3-FRB	Y'	2.48 ± 0.19	3	-0.27	0.1962

b

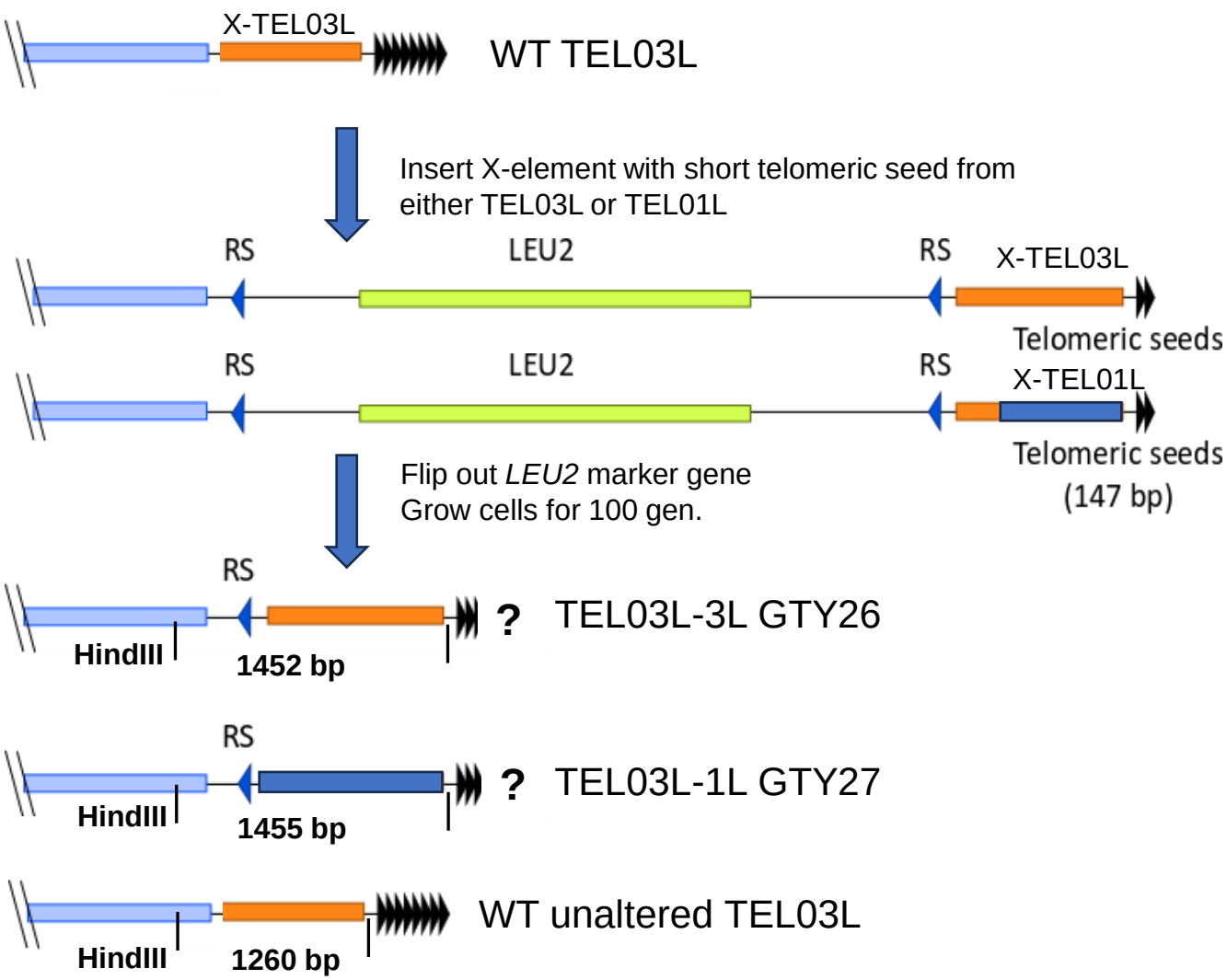

Figure 3

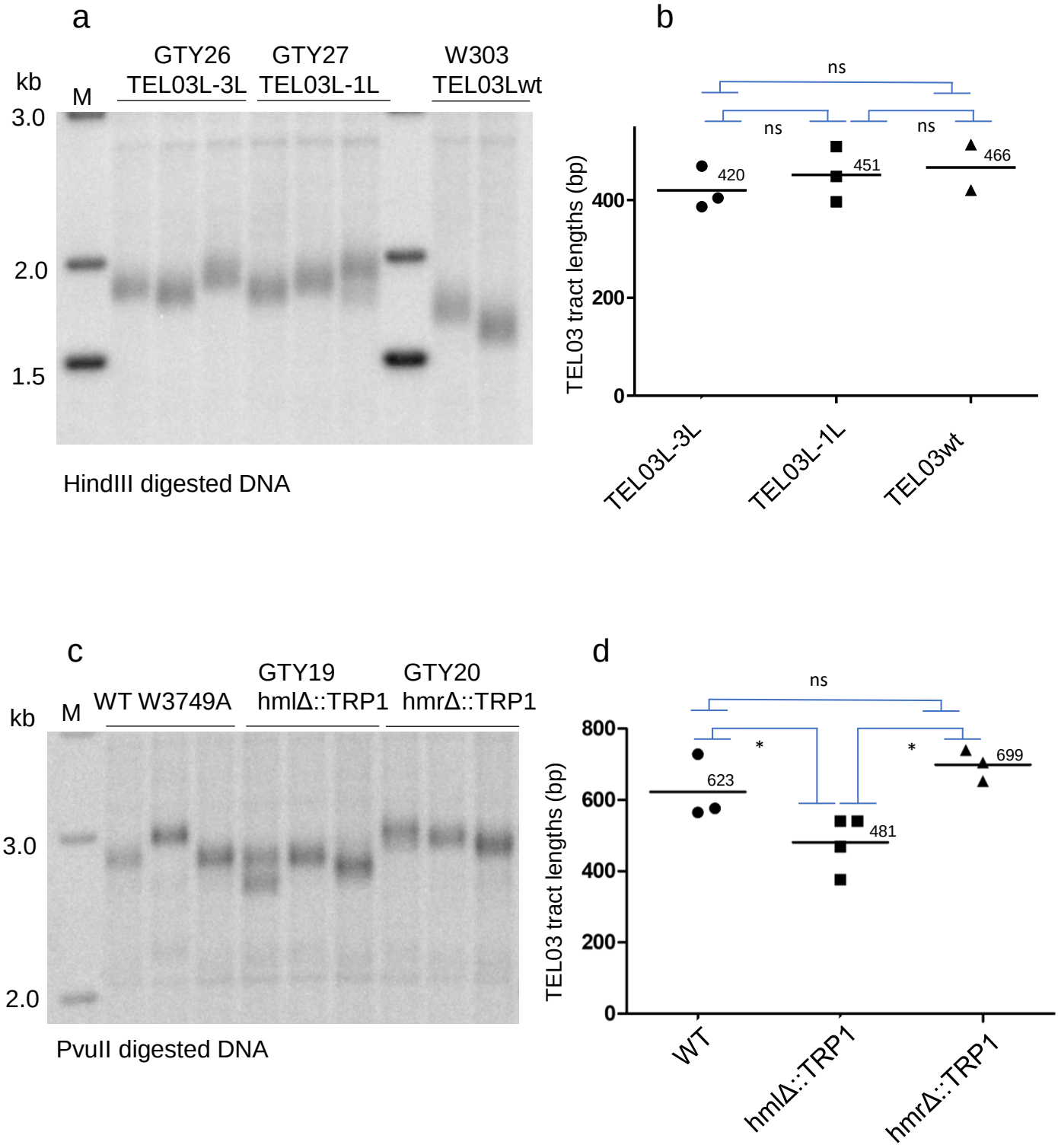
a
kb
M
GTY26
TEL03L-3L
GTY27
TEL03L-1L
W303
TEL03Lwt
3.0
2.0
1.5
HindIII digested DNA
b
ns
ns
ns
420
451
466
TEL03 tract lengths (bp)
400
200
0
TEL03L-3L
TEL03L-1L
TEL03wt
c
kb
M
WT W3749A
GTY19
hmlΔ::TRP1
GTY20
hmrΔ::TRP1
3.0
2.0
PvuII digested DNA
d
ns
*
*
623
481
699
TEL03 tract lengths (bp)
800
600
400
200
0
WT
hmlΔ::TRP1
hmrΔ::TRP1

Extended Figure 3

a

1

Telomere	Mean ± SD	n	Difference with TEL03L (WT)		Difference with TEL03L (TEL03L-3X)	
			Mean difference	P-value	Mean difference	P-value
TEL03L-3L	419.66 ± 43.66	3	-46.84	0.3972		
TEL03L-1L	451 ± 56.55	3	-15.5	0.7949	-31.34	0.4898
TEL03L (WT)	466.5 ± 65.76	2				

2

Gen.	Telomere	Mean +/- SD	n	Difference with TEL03L (WT)		Difference with TEL03L *(hmlΔ)*	
				Mean difference	P-value	Mean difference	P-value
W3749A (WT)	TEL03L	623 ± 91.09	3			141.75	0.0254*
hmlΔ	TEL03L	481.25 ± 77.74	3	-141.75	0.0254*		
hmrΔ	TEL03L	699.33 ± 43.77	3	76.33	0.5963	218.08	0.0141*

b

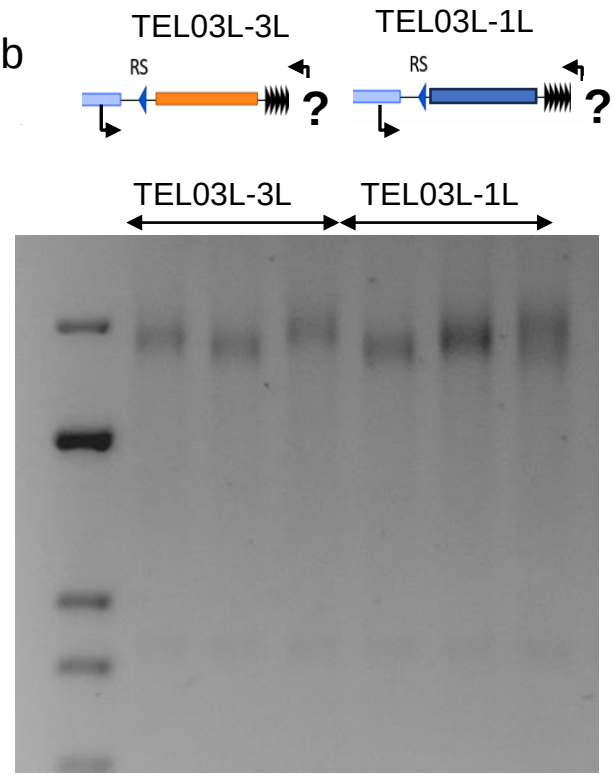

Telo. Rep. (bps) 531 487 549 475 512 562

c

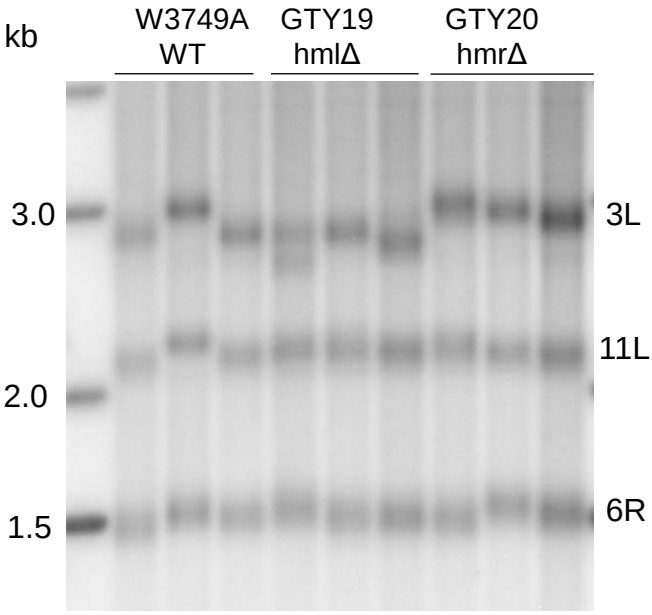

PvuII digested DNA

d

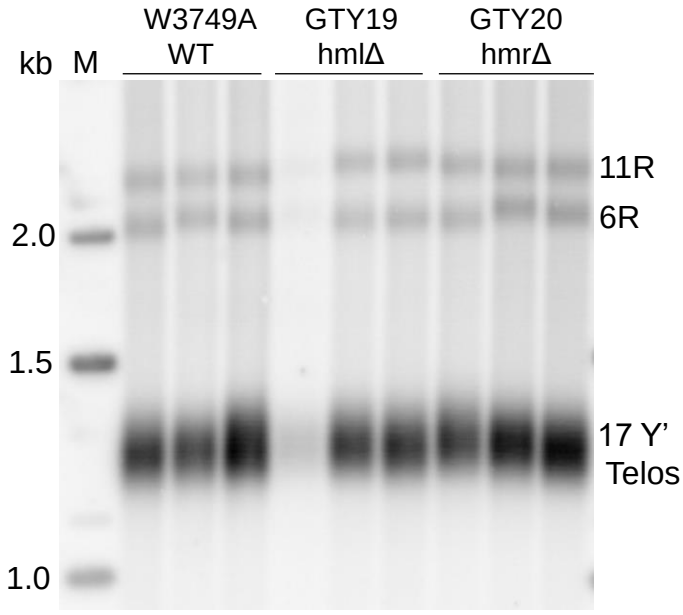

XhoI digested DNA

Figure 4

a

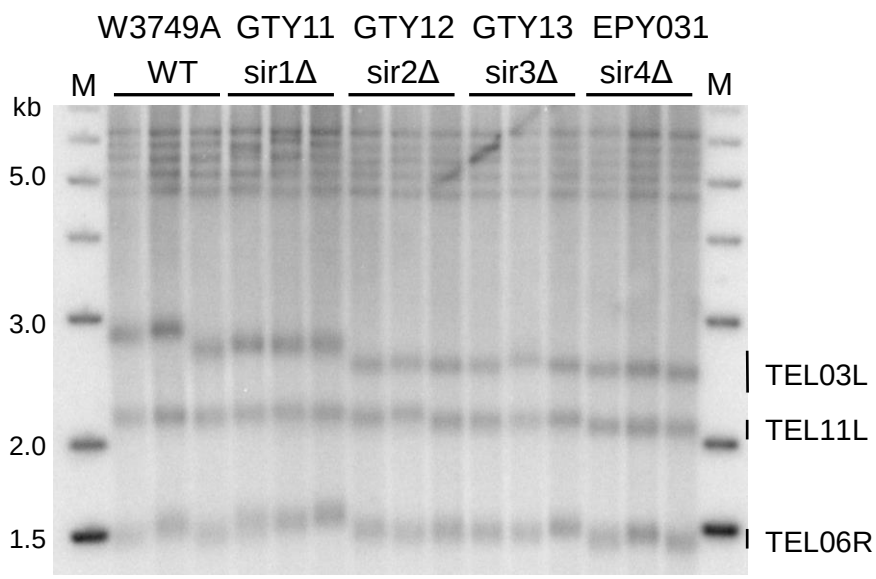

PvuII digested DNA

b

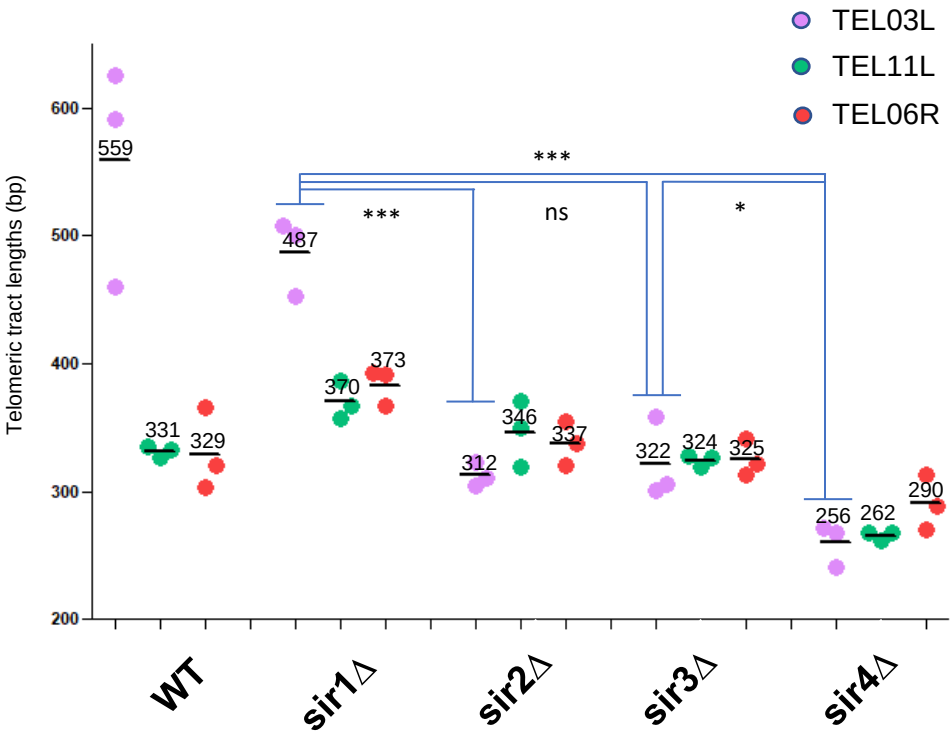

Extended Figure 4

a

Telomere	Genotype	Mean ± SD	n	Difference with WT strain	
				Mean difference	P-value
TEL03L	**W3749A (WT)**	558.7 ± 87.12	3		
TEL03L	***sir1Δ***	486 ± 30.28	3	-72.7	0.2478
TEL03L	***sir2Δ***	312.3 ± 9.71	3	-246.4	0.0082
TEL03L	***sir3Δ***	321.7 ± 31.56	3	-237	0.0114
TEL03L	***sir4Δ***	256.33 ± 13.6	3	-302.37	0.0043
TEL11L	**W3749A (WT)**	331 ± 4.58	3		
TEL11L	***sir1Δ***	370 ± 14.73	3	39	0.0119
TEL11L	***sir2Δ***	346.33 ± 25.69	3	15,33	0.3665
TEL11L	***sir3Δ***	324 ± 4.35	3	-7	0.1277
TEL11L	***sir4Δ***	261.66 ± 5.03	3	-69,34	< 0.0001
TEL06R	**W3749A (WT)**	329.33 ± 32.03	3		
TEL06R	***sir1Δ***	373.33 ± 7.09	3	44	0.0558
TEL06R	***sir2Δ***	337 ± 17	3	7.67	0.7328
TEL06R	***sir3Δ***	325.33 ± 14.29	3	-4	0.853
TEL06R	***sir4Δ***	290.33 ± 21.59	3	-39	0.1553

b

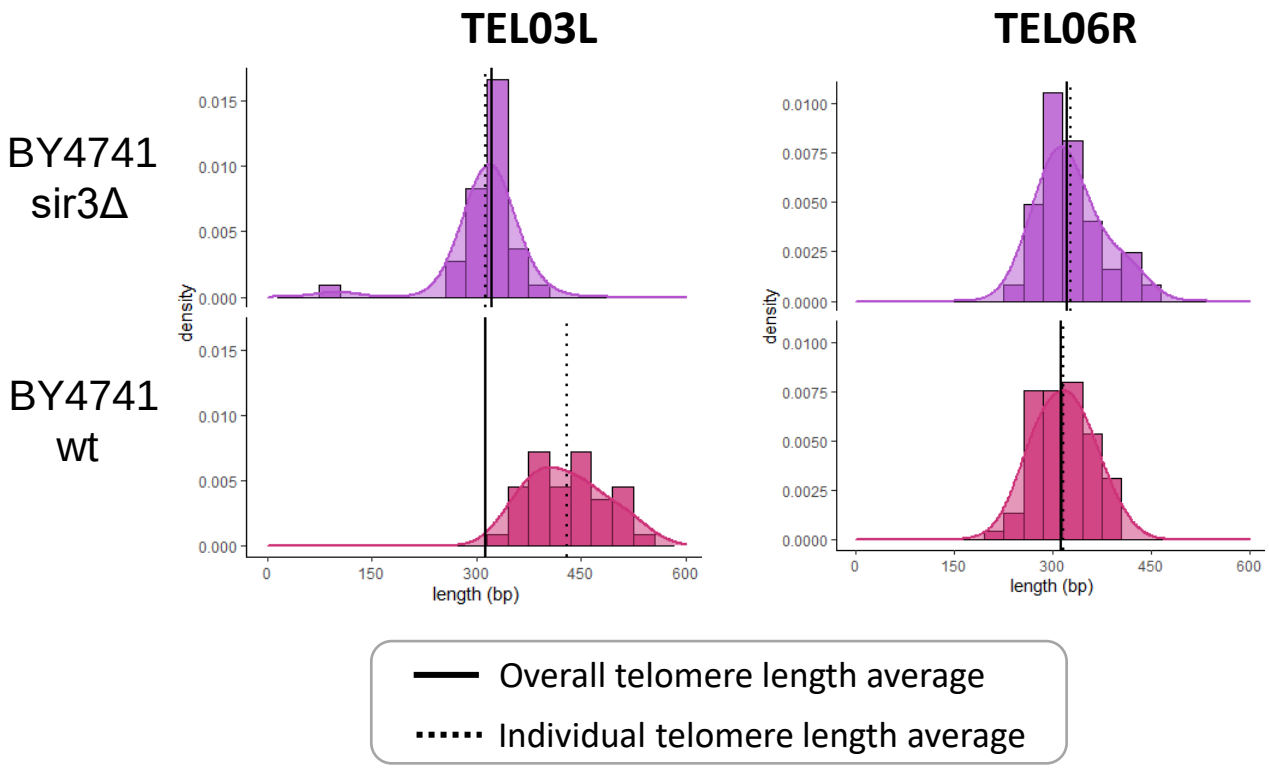

Figure 5

a

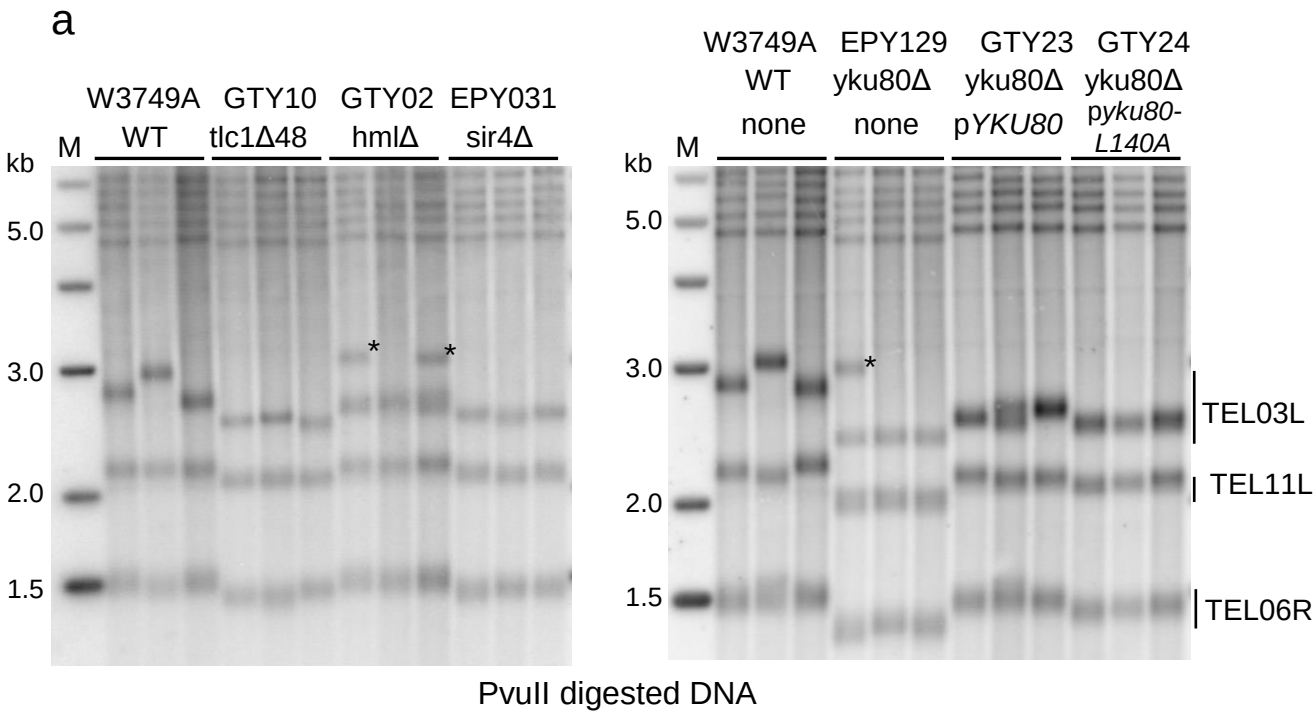
W3749A
WT
GTY10
tlc1Δ48
GTY02
hmlΔ
EPY031
sir4Δ
M
kb
5.0
3.0
2.0
1.5
*
*
W3749A
WT
none
EPY129
yku80Δ
none
GTY23
yku80Δ
pYKU80
GTY24
yku80Δ
pyku80-
L140A
M
kb
5.0
3.0
2.0
1.5
*
TEL03L
TEL11L
TEL06R
PvuII digested DNA

b

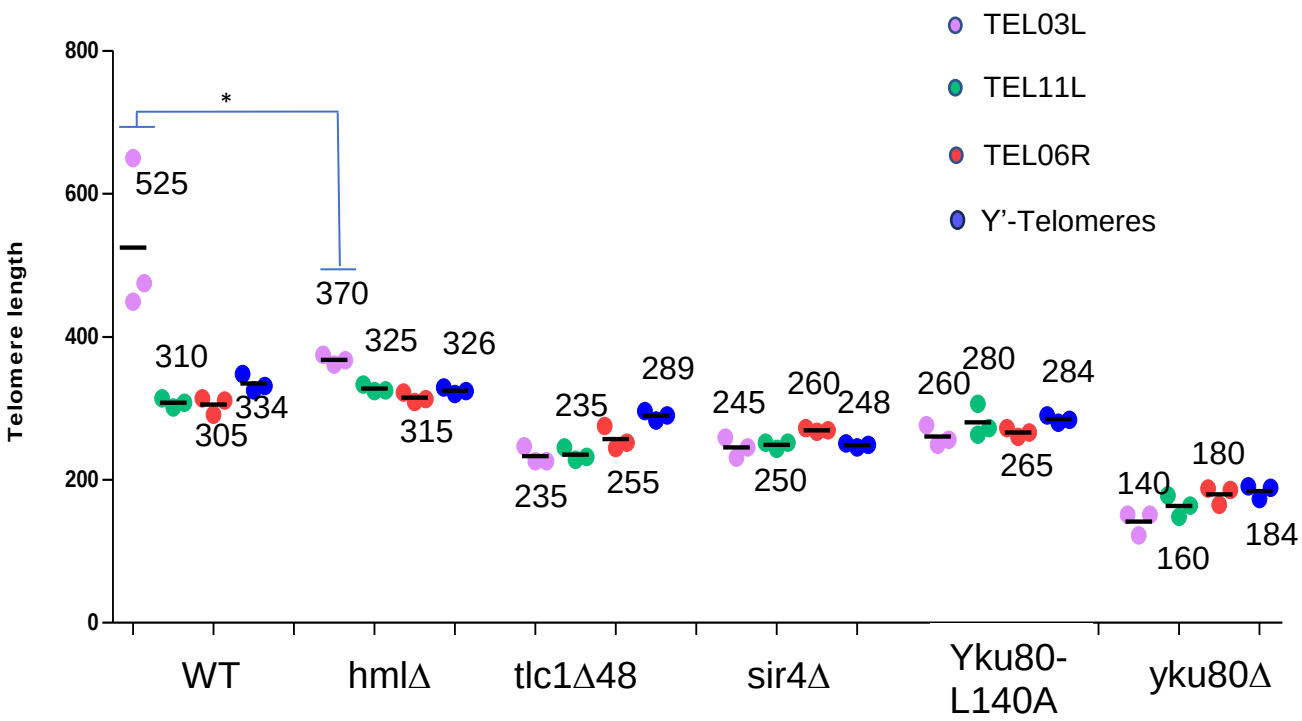
TEL03L
TEL11L
TEL06R
Y'-Telomeres
Telomere length
800
600
400
200
0
*
525
370
310
305
334
325
315
326
235
235
255
289
245
250
260
248
260
265
280
284
140
160
180
184
WT
hmlΔ
tlc1Δ48
sir4Δ
Yku80-
L140A
yku80Δ

Extended Figure 5

a

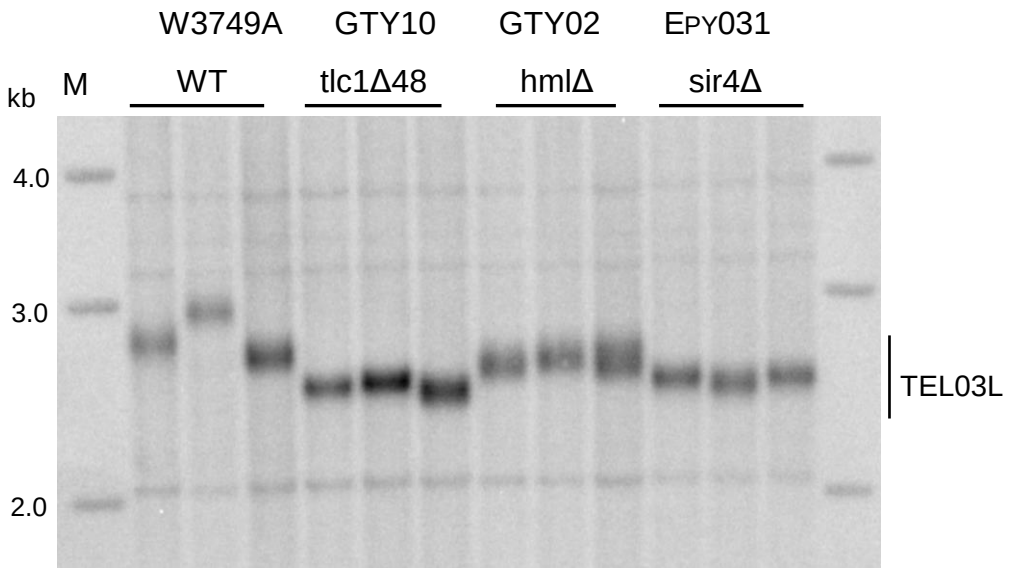

PvuII digested DNA

b

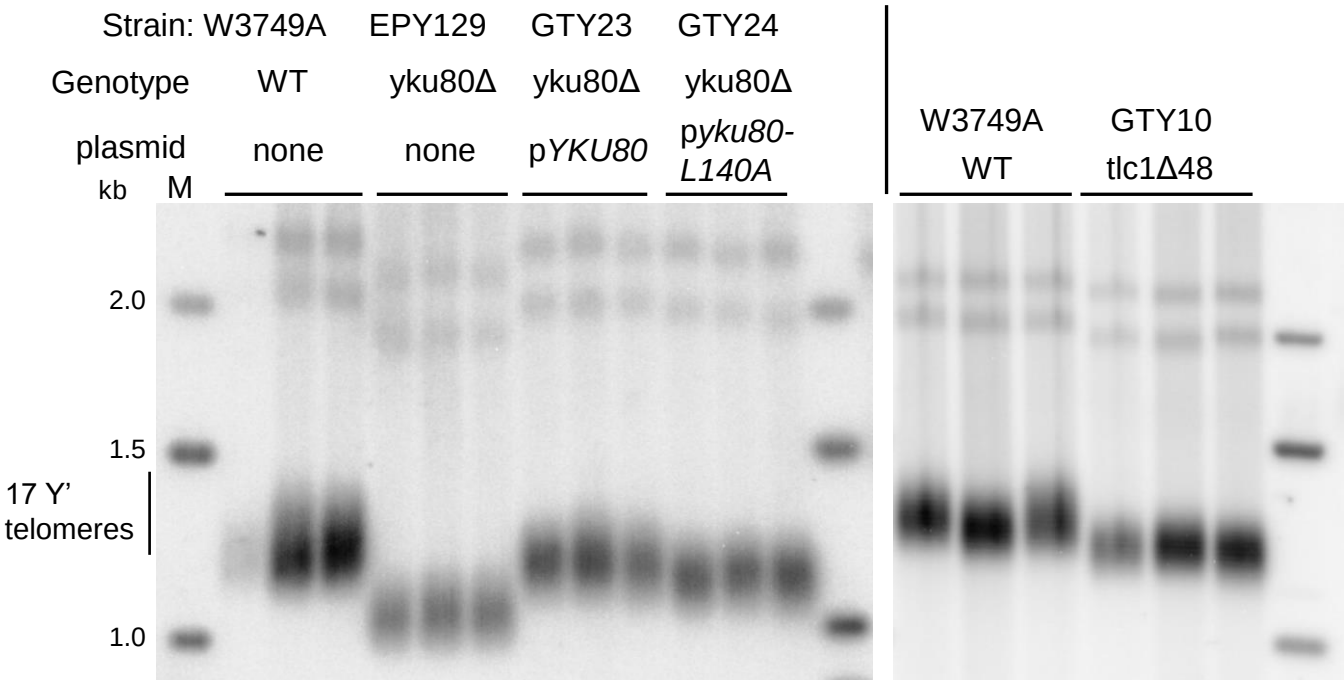

XhoI digested DNA

Extended Figure 5, continued

c

1

Telomere	Genotype	Mean ± SD	n	Difference with WT strain	
				Mean difference	P-value
TEL03L	**W3749A (WT)**	524.66 ± 109.31	3		
TEL03L	***tlc1Δ48***	233 ± 12.12	3	-291.66	0.0168
TEL03L	***hmlΔ***	367.66 ± 7.02	3	-157	0.0685
TEL03L	***sir4Δ***	245 ± 14	3	-279.66	0.0181
TEL11L	**W3749A (WT)**	307.66 ± 6.05	3		
TEL11L	***tlc1Δ48***	235 ± 8.88	3	-72.66	0.0002
TEL11L	***hmlΔ***	327.33 ± 4.93	3	19.67	0.2535
TEL11L	***sir4Δ***	249 ± 5.19	3	-58.66	0.0241
TEL06R	**W3749A (WT)**	305.33±12.50	3		
TEL06R	***tlc1Δ48***	257±16.09	3	-48.33	0.0086
TEL06R	***hmlΔ***	314.66±6.65	3	9.33	0.535
TEL06R	***sir4Δ***	269.33±2.51	3	-36	0.0063

2

Telomere	Genotype	Mean ± SD	n	Difference with WT strain	
				Mean difference	P-value
TEL03L	**W3749A (WT)**	608 ± 117.47	3		
TEL03L	***yku80Δ***	141.33 ± 16.74	3	-466.67	0.0024
TEL03L	***yku80Δ + pYKU80-myc***	327 ± 38.43	3	-281	0.0017
TEL03L	***yku80Δ + pyku80-L140A-myc***	260.33 ± 14.01	3	-347.67	0.0007
TEL11L	**W3749A (WT)**	351.66 ± 36.11	3		
TEL11L	***yku80Δ***	163.33 ± 15.01	3	-188.33	0.0011
TEL11L	***yku80Δ + pyku80-myc***	312.66 ± 13.01	3	-39	0.1533
TEL11L	***yku80Δ + pYKU80-L140A-myc***	280.33 ± 22.67	3	-71.33	0.0442
TEL06R	**W3749A (WT)**	311.33 ± 14.50	3		
TEL06R	***yku80Δ***	179.66 ± 12.74	3	-131.67	0.0003
TEL06R	***yku80Δ + pYKU80-myc***	301 ± 11.13	3	-10.33	0.3831
TEL06R	***yku80Δ + pyku80-L140A-myc***	266 ± 22.6	3	-45.33	0.0075

Figure 6

a

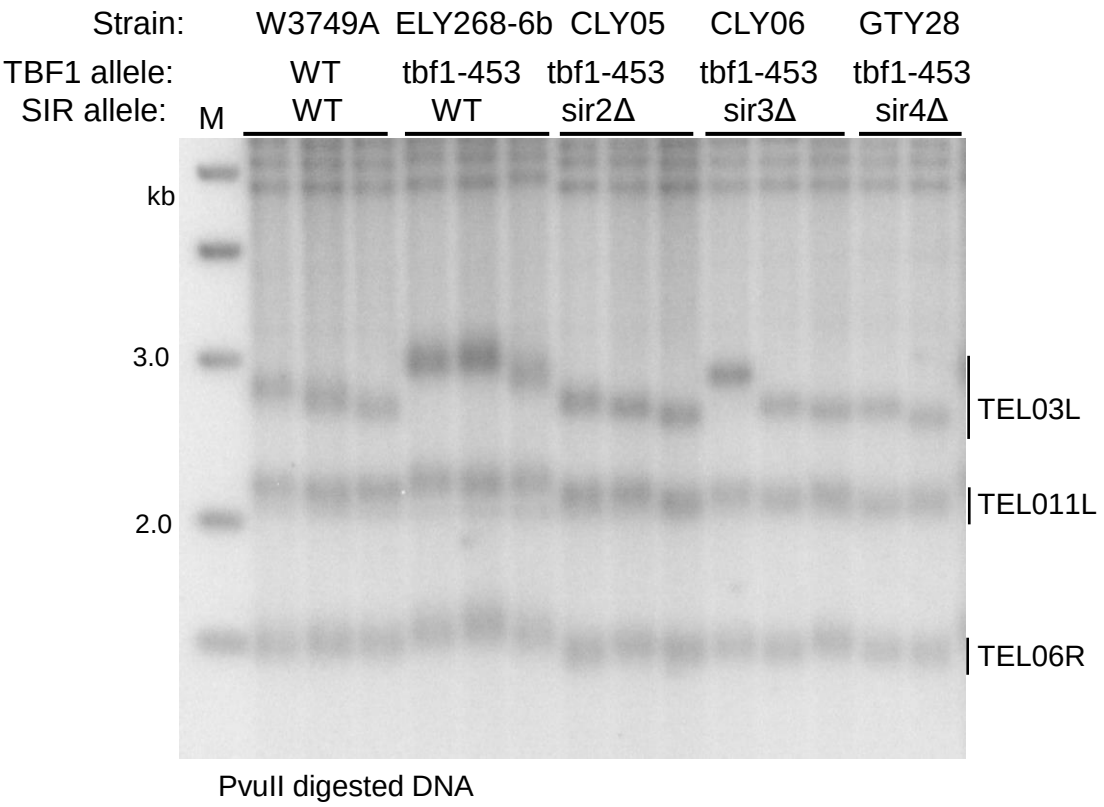
Strain:
W3749A
ELY268-6b
CLY05
CLY06
GTY28
TBF1 allele:
WT
tbf1-453
tbf1-453
tbf1-453
tbf1-453
SIR allele:
M
WT
WT
sir2Δ
sir3Δ
sir4Δ
kb
3.0
2.0
TEL03L
TEL011L
TEL06R
PvuII digested DNA

b

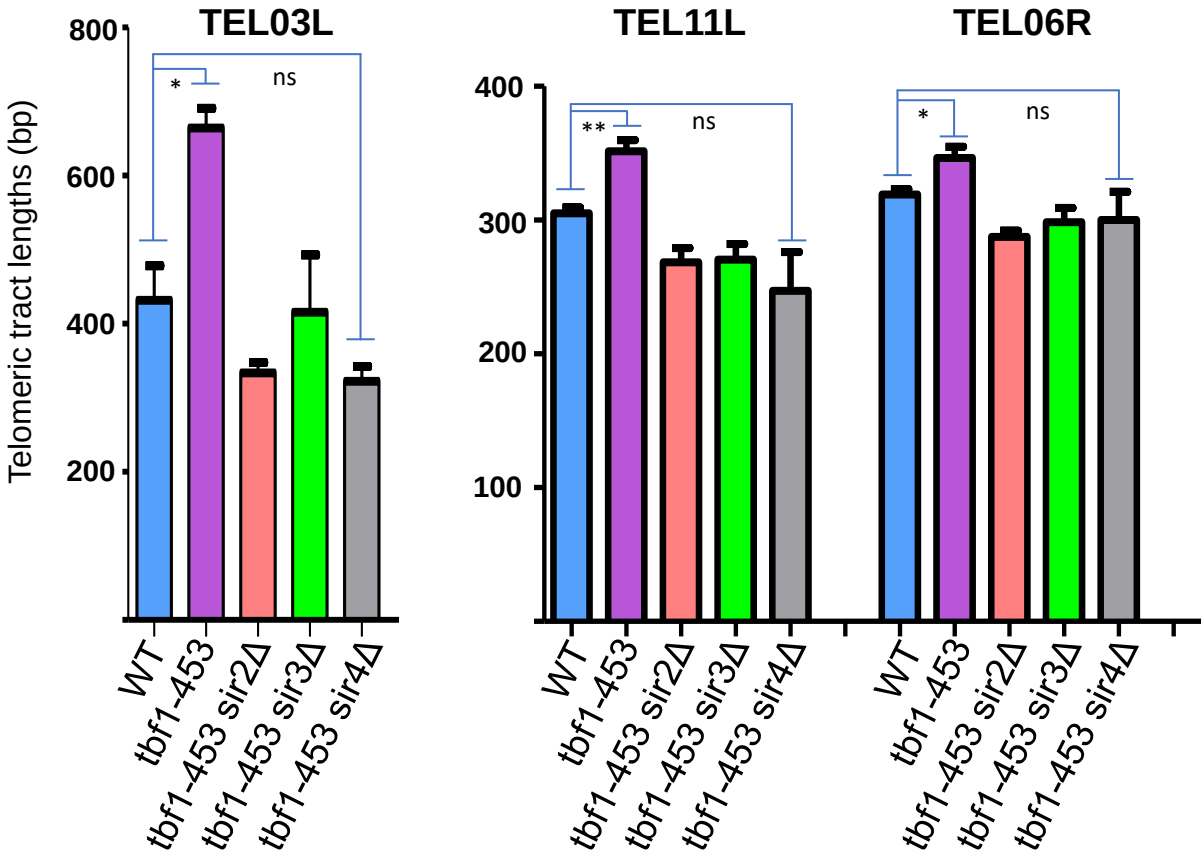
TEL03L
TEL11L
TEL06R
Telomeric tract lengths (bp)
800
600
400
200
400
300
200
100
*
ns
**
ns
*
ns
WT
tbf1-453
tbf1-453 sir2Δ
tbf1-453 sir3Δ
tbf1-453 sir4Δ

Extended Figure 6

a

b

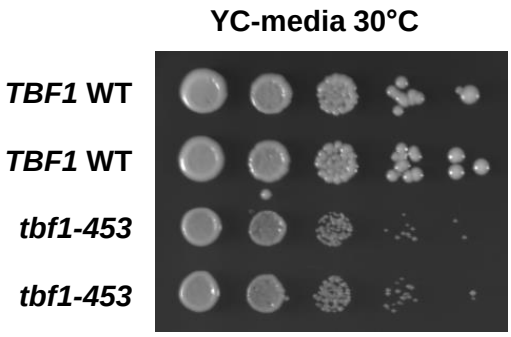

c

WT vs *tbf1-453* 30°C; total RNA seq	
RNAs (+) = Tbf1 binding site in promoter (-) = no Tbf1 binding site	**Log2-ratio**
TBF1 (+)	1.1
PAF1 (+)	0.9
HAC1 (+)	1.2
PUF6 (-)	0.6
SNR190 (+)	-0.8
SNR85 (-)	1.7
Telomeric mRNAs	
SIR1	1.3
SIR2	0.4
SIR3	1.5
SIR4	1.1
RIF1	1.2
RIF2	0.4
EST1	1.8
EST2	1.7

d

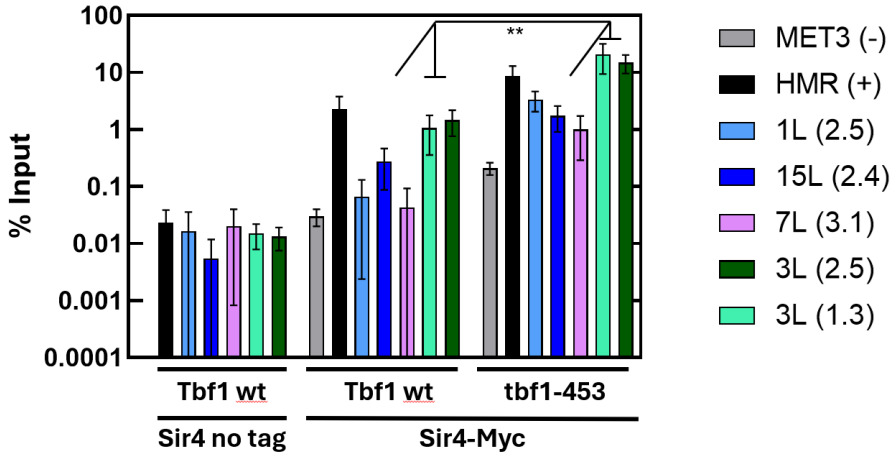

Extended Figure 7

a

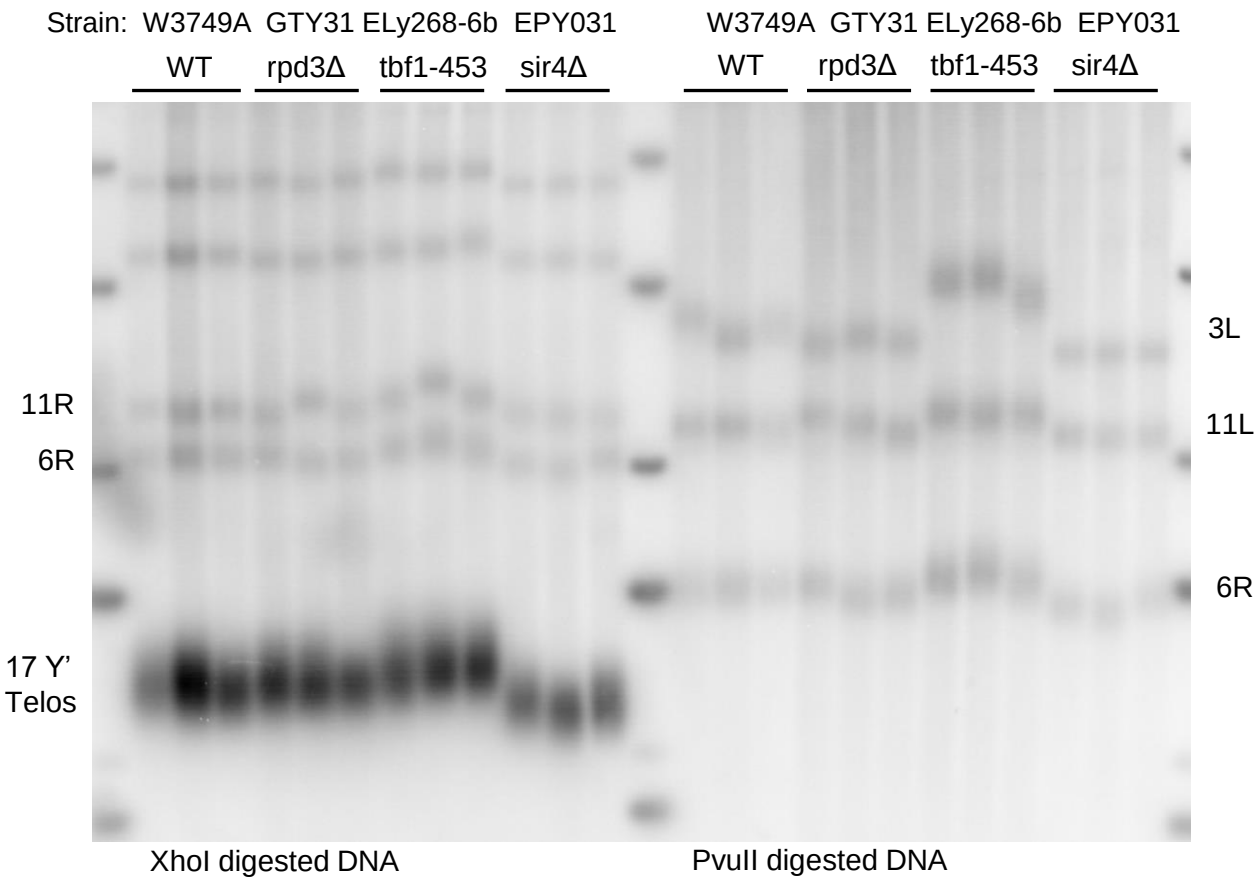

b

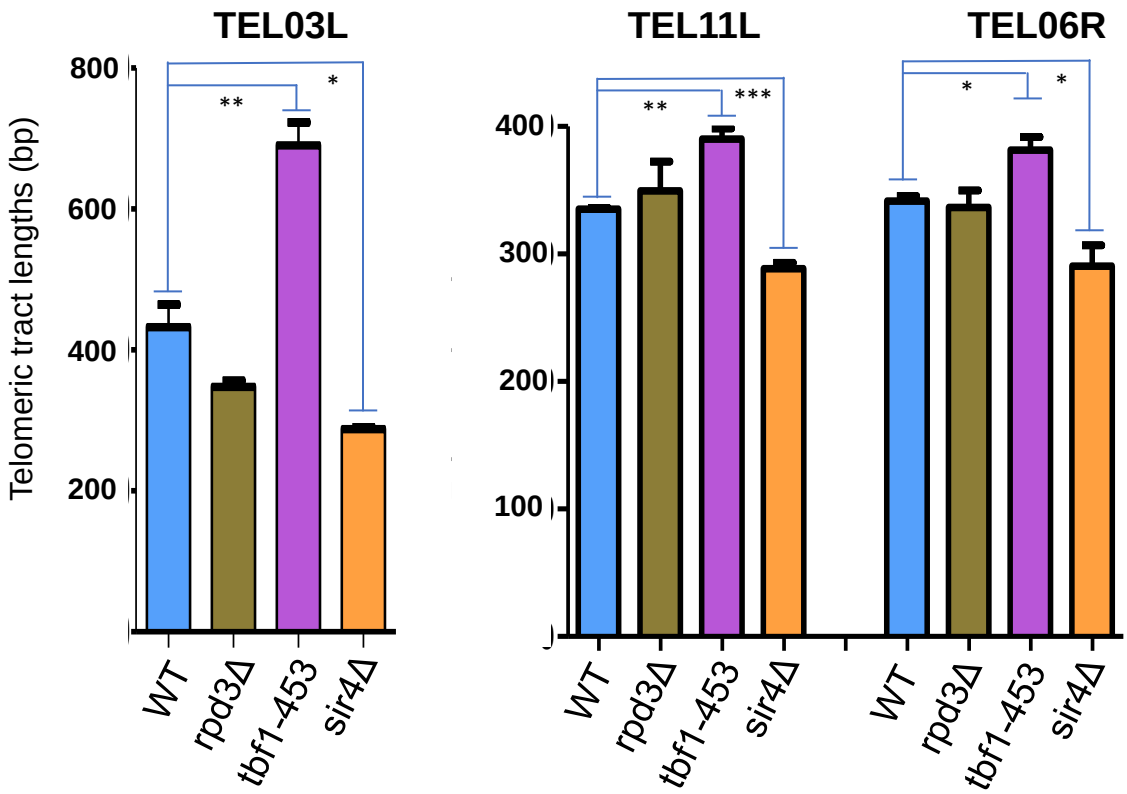

Extended Figure 7, continued

c

1

Telomere	Genotype	Mean ± SD	n	Difference with WT strain	
				Mean difference	P-value
TEL03L	**W3749A (WT)**	431.66 ± 80.57	3		
TEL03L	***tbf1-453***	664 ± 47.14	3	232.34	0.0125
TEL03L	***tbf1-453 sir2Δ***	333.33 ± 25.14	3	-98.33	0.1138
TEL03L	***tbf1-453 sir3Δ***	415.66 ± 133.70	3	-16	0.86
TEL03L	***tbf1-453 sir4Δ***	322 ± 28.28	3	-109.66	0.1745
TEL11L	**W3749A (WT)**	305 ± 7.54	3		
TEL11L	***tbf1-453***	352.66 ± 14.18	3	47.66	0.0073
TEL11L	***tbf1-453 sir2Δ***	268.33 ± 18.47	3	-36.67	0.035
TEL11L	***tbf1-453 sir3Δ***	270.33 ± 20.42	3	-34.67	0.051
TEL11L	***tbf1-453 sir4Δ***	288 ± 76.70	3	-17	0.72
TEL06R	**W3749A (WT)**	319 ± 7	3		
TEL06R	***tbf1-453***	346.33 ± 14.97	3	27.33	0.0458
TEL06R	***tbf1-453 sir2Δ***	287.66 ± 8.08	3	-31.34	0.0071
TEL06R	***tbf1-453 sir3Δ***	298.33 ± 19	3	-20.67	0.152
TEL06R	***tbf1-453 sir4Δ***	300 ± 36.37	3	-19	0.42

2

Telomere	Genotype	Mean ± SD	n	Difference with WT strain	
				Mean difference	P-value
TEL03L	**W3749A (WT)**	432 ± 56.55	3		
TEL03L	***rpd3Δ***	347.66 ± 14.57	3		
TEL03L	***tbf1-453***	690.33 ± 57.13	3	258.33	0.0051
TEL03L	***sir4Δ***	287.66 ± 4.04	3	-144.34	0.0116
TEL11L	**W3749A (WT)**	335 ± 1.73	3		
TEL11L	***tbf1-453***	349.33 ± 40.01	3		
TEL11L	***tbf1-453 sir2Δ***	390 ± 15	3	55	0.0032
TEL11L	***tbf1-453 sir3Δ***	288.33± 8.62	3	-46.67	0.0008
TEL06R	**W3749A (WT)**	341.66 ± 6.80	3		
TEL06R	***tbf1-453***	336.33 ± 23.11	3		
TEL06R	***tbf1-453 sir2Δ***	381.33 ± 18	3	39,67	0.0234
TEL06R	***tbf1-453 sir3Δ***	290.33 ± 28.71	3	-51,33	0.0394